HHS Public Access

Author manuscript

J Sound Vib. Author manuscript; available in PMC 2016 January 04.

Published in final edited form as:

J Sound Vib. 2015 November 10; 356: 195–216. doi:10.1016/j.jsv.2015.06.047.

Theoretical foundation, methods, and criteria for calibrating human vibration models using frequency response functions

Ren G. Dong[*], **Daniel E. Welcome**, **Thomas W. McDowell**, and **John Z. Wu**

Engineering & Control Technology Branch, National Institute for Occupational Safety and Health, Morgantown, WV 26505, USA

Abstract

While simulations of the measured biodynamic responses of the whole human body or body segments to vibration are conventionally interpreted as summaries of biodynamic measurements, and the resulting models are considered quantitative, this study looked at these simulations from a different angle: model calibration. The specific aims of this study are to review and clarify the theoretical basis for model calibration, to help formulate the criteria for calibration validation, and to help appropriately select and apply calibration methods. In addition to established vibration theory, a novel theorem of mechanical vibration is also used to enhance the understanding of the mathematical and physical principles of the calibration. Based on this enhanced understanding, a set of criteria was proposed and used to systematically examine the calibration methods. Besides theoretical analyses, a numerical testing method is also used in the examination. This study identified the basic requirements for each calibration method to obtain a unique calibration solution. This study also confirmed that the solution becomes more robust if more than sufficient calibration references are provided. Practically, however, as more references are used, more inconsistencies can arise among the measured data for representing the biodynamic properties. To help account for the relative reliabilities of the references, a baseline weighting scheme is proposed. The analyses suggest that the best choice of calibration method depends on the modeling purpose, the model structure, and the availability and reliability of representative reference data.

1. Introduction

The characterization of human vibration biodynamics is important for understanding vibration effects and for assessing the risks of vibration exposures [1–5]. The biodynamic responses are basically a passive mechanical process, similar to the responses of many engineering structures to vibration. In engineering, the model of a system is usually constructed using a forward dynamic approach, in which the dynamic properties of the system are directly measured and used in the model to predict the dynamic responses. Because it is difficult to directly measure the biodynamic properties of living human

[*]Correspondence to: ECTB/HELD/NIOSH/CDC, 1095 Willowdale Road, MS L-2027, Morgantown, WV 26505, USA. Tel.: +1 304 285 6332; fax: +1 304 285 6265. rkd6@cdc.gov (R.G. Dong).

Disclaimer

The findings and conclusions in this report are those of the authors and do not necessarily represent the official position of the National Institute for Occupational Safety and Health.

subjects, human vibration models are most frequently constructed using an inverse dynamic approach or a hybrid forward and inverse approach [6–12]. The inverse approach estimates the unknown biodynamic properties of a model using the measured time-history responses (forces and motions) and/or frequency response functions (apparent mass, mechanical impedance, and vibration transmissibility) of the system. Mathematically, the property parameters are determined by imposing matches between modeled responses/functions and the corresponding measured responses/functions. In principle, this imposed matching process passes the dynamic properties included in the reference data to the model, similar to the calibration of an accelerometer. In engineering modeling, this process is usually termed as parameter identification, as it is only used to identify the unknown values of one or a few well-defined parameters of a model that provides a close simulation of an engineering system [13,14]. In contrast, the vast majority of human vibration models are lumped-parameter models that only provide a very crude simulation of the complex human body structure. The exact physical representations of some model components are not known or predetermined before their values are identified. Their representations are actually interpreted according to their values. As a result, the components in the same model structure may represent different parts or properties of the human body or segment, depending on the characteristics of the reference functions used in the modeling, as observed in our previous studies [9,15]. Therefore, this process not only calibrates the values of the model parameters, but it may also calibrate the physical meanings of some model components. It may be more appropriate to refer to this process as model calibration in human vibration modeling.

Such model calibration makes it possible for many researchers to efficiently construct human vibration models for understanding the basic characteristics and motion mechanisms of human biodynamic responses using inexpensive modeling techniques. This further explains why the vast majority of human vibration models have been developed using this approach. Such models are also adequate and efficient for enhancing the designs, analyses, and evaluations of tools, seats, and anti-vibration devices [16–18], and/or for constructing test apparatuses or human test dummies [19,20]. To help further understand vibration effects and to help assess the risks of vibration exposures, it is required to improve such models for better predictions and understanding of the biodynamic responses in the human body. A major deficiency of the reported lumped-parameter models is that they may not be used to predict the dynamic forces at many joints and the vibration power absorption distributed in different tissues, as these models do not provide a reasonable simulation of the relationships among the bones, joints and soft tissues. Although vibration is likely to be primarily transmitted through the bones and joints, these structures only account for less than 20 percent of the body mass [21]; the soft tissues account for the vast majority of the body mass and are thus likely to play a major role in determining the overall responses, according to a recently derived theorem [22]. While it is not difficult to configure a model that separately simulates the bones, joints, and soft tissues, it remains a formidable research task to determine how such models can be reliably calibrated and reasonably validated. Enhancing the understanding of model calibration may accelerate the development of such models.

Based on function, human vibration models are conventionally classified into three categories: mechanistic, quantitative, and effects models [23]. A set of validation criteria and

a checklist for the models in each category have also been proposed [23]. Because these criteria are not based on the concept of model calibration, they do not systemically and directly address the technical issues and requirements of the model development using the inverse dynamic approach. Instead, the human vibration modeling society generally interprets model calibrations only as quantitative summaries of biodynamic measurements [23], similar to the statistical regressions used in the analyses of experimental data. According to such limited understanding, the majority of the reported human vibration models are classified as quantitative models [23]. Such a classification actually incorrectly considers the quantitative summaries as the final function of these models, as the endpoints of these models are not the quantitative summaries but they are primarily for the above-mentioned applications. This classification also contradicts the major purposes of such computer modeling – to predict the responses or parameters that cannot be directly measured and/or to understand the phenomena that cannot be easily understood from the experimental data themselves. Another questionable practice is that, according to how quantitative models are defined, these models are often considered to be validated as long as they can provide a good curve fit to a set of measured data. Because there is no uniform specification for judging the goodness of curve fitting in human vibration modeling, many studies have portrayed their models as being validated simply because those models reflect the study's best curve fits; there is often insufficient assessment of the model's ability to represent the targeted biodynamic properties or response functions. Such a practice is problematic for the following reasons: (i) the best curve fitting can always be achieved for any experimental data on any model, even if its equations of motion include serious errors, as observed in a recently reported study [24]; (ii) the best curve fitting can also be achieved even if the reference functions include significant errors, and/or the transmissibility measured on one substructure is used to represent the vibrations of other substructures, which are also observed in the reported study [24]. Obviously, more effective validation criteria that directly address these issues are required for the further development and evaluation of human vibration models.

Also because there is lack of understanding of model calibration, it is not clear how to appropriately select and apply the specific calibration schemes. While apparent mass or impedance has been used to calibrate some models [7–9], vibration transmissibility has been used to calibrate some other models [10,25,26]. However, more researchers have used both transmissibility and driving-point response functions [6,24,27]. Some of these researchers hypothesized that such a combination would provide a more reliable calibration [24,27]. The current study hypothesized that the best choice of the calibration method depends on many factors, which may include the specific application of the model, the model structure, and the availability and reliability of the reference functions. Further studies are required to test these hypotheses.

In many cases, it is difficult to clearly differentiate or categorize these models, especially the mechanistic and quantitative models, as they usually both include mechanistic and quantitative components. Even though some finite element models were originally developed using the forward modeling approach, some of the element properties have to be adjusted through model calibration so that the modeling predictions can be more reliable [11,28]; the biodynamic properties are usually measured with cadaver tissues that may not

be fully representative of live subject properties, and the individual differences may further increase the complexities and difficulties. On the other hand, some models were originally developed to simulate the biodynamic measurements, but they can be considered as mechanistic models after their parameters are understood and can be physically associated with the specific substructures of the human body or segments [9,15]. As such merging marks the advancement of modeling knowledge [23], the hybrid forward and inverse dynamic approach is likely to be more frequently used in the future. It is important to formulate the calibration validation criteria that are generally applicable to models in every category.

Based on this background, the specific aims of this study are to review and enhance the theoretical foundation for human model calibration, to systematically examine the calibration methods, to identify their basic criteria and requirements, and to explore the improvements of the calibration methods. This study also proposed some new interpretations of the reported models.

2. Basic theory and methodology

Fig. 1 shows a flowchart that outlines the theoretical basis and major activities of this study. Similar to the forward dynamic approach, the inverse dynamic approach can be applied to any model with linear or nonlinear dynamic properties [6–14]. The human body or segment has some nonlinear properties. For example, the stiffness of the body tissues generally increases with the increase in applied forces or the force-induced tissue deformation [29]; as a result, the resonant frequency of the human hand – arm system increases with applied hand forces [30]. The biodynamic responses of the human body may also involve in some nonlinear processes. For example, driven by a large shock or vibration, a body or hand may lose or partially lose contact with a seat or handle. Because of these nonlinear features, the fundamental resonant frequency of the whole body generally reduces with the increase in vibration magnitude [1]. However, to make the modeling analysis efficient and less technically demanding, the human body or segment is most frequently simulated as a linear system without considering the nonlinear processes. This is acceptable for many of the above-mentioned applications. Furthermore, a linear model can also be used to identify the nonlinear properties of the system, which may be further used to construct a nonlinear model and to simulate the nonlinear processes. For example, the palm of the hand exhibits nonlinear contact stiffness and damping characteristics that are very difficult to directly measure. These properties can be locally linearized for each given push force. A model with linear parameters can be used to calibrate the linear stiffness and damping parameters using the experimental data measured under each push force [31]. Then, the parameter values for different push forces can be used to determine the nonlinear characteristics of these parameters. The results can be used to replace the linear stiffness and damping properties in the model to establish a nonlinear model. To efficiently analyze and discuss the model calibration methods, this study generally assumed the human body or segment can be approximately simulated as a linear system for each given test condition, although the inverse dynamic approach is generally applicable to any linear and nonlinear system [7,9,13,14]. Six models found in the literature are shown in Fig. 2 [7–9,18,21]. They were used in this study not only because they are simple for evaluation but also because they have

different structural features and can be used to help identify the requirements of a unique solution for each calibration method. They were also used as examples to help efficiently describe and demonstrate the applications of the study methods and proposed validation criteria. While the model parameters are defined in the figures, their values found in the literature are listed in Table 1.

2.1. Equations of motion and general calibration procedures

The first step to develop a new model is to select or design the model structure based on the purpose or application of the model. Then, according to Newton's second law, the equations of motion for the model can be written in a general matrix form as follows [32]:

$$\mathbf{M}\ddot{\mathbf{u}}+\mathbf{C}\dot{\mathbf{u}}+\mathbf{K}\mathbf{u}=\mathbf{M_0}\ddot{\mathbf{u}}_0+\mathbf{C_0}\dot{\mathbf{u}}_0+\mathbf{K_0}\mathbf{u}_0, \quad (1)$$

where **M** is mass matrix, **C** is damping matrix, and **K** is stiffness matrix, **u** (=x_1, x_2, …, x_n, … z_1, z_2, …, z_n) is the coordinate vector, $\mathbf{u_0}$ (=x_0, …, z_0) is the coordinate vector of the foundation in motion, $\mathbf{M_0}$, $\mathbf{C_0}$, and $\mathbf{K_0}$ are the mass matrix, damping matrix, and stiffness matrix, respectively related to the motion of the foundation.

To help efficiently describe the general calibration procedures, this study assumes that any system mentioned in the following presentation is excited by a single steady-state vibration $(\ddot{u}_0)$ from the foundation in motion, which can be expressed as follows:

$$\ddot{u}_0=\ddot{U}_0 \cdot \exp^{j\omega t}, \quad (2)$$

where $\ddot{U}_0$ is vibration magnitude (m/s^2), $j=\sqrt{-1}$, ω is circular frequency (Rad/s), and t is time (s).

This study also assumes that χ is the vector of unknown parameters (P_{u1}, P_{u2}, …, P_{ui}, … P_{un}) of the model to be calibrated. For example, if all the parameters of Model-(e) shown in Fig. 2(e) are unknown or will be determined from the calibration, χ=(m_{01}, m_{02}, m_1, m_2, c_1, c_2, c_3, c_4, k_1, k_2, k_3, k_4). The objective of the model calibration is to determine these parameters. The specific procedures for parameter determinations may vary among the reported studies [6–12,27]. These procedures can be generally outlined as follows:

- The reference functions are collected or measured from human subject experiments.
- The modeling motion responses (**u**) are calculated by assuming an excitation $(\ddot{u}_0)$ and an initial value for each unknown parameter in its constrained range using Eq. (1). A preliminary constrained range (e.g., > 0) for each parameter may be determined based on available knowledge of the parameter. It may be refined after the preliminary calibration results are obtained and understood.
- The vibration transmissibility (VT) functions $(\mathbf{T}=\ddot{\mathbf{u}}/\ddot{u}_0)$, the dynamic force on the foundation of motion ($\mathbf{F}_0$), and the driving-point response function (DPR) such as the apparent mass $(\mathbf{M_A}=\mathbf{F}_0/\ddot{u}_0)$ or mechanical impedance $(\boldsymbol{Z}=j\omega \cdot \mathbf{F}_0/\ddot{u}_0)$ are

calculated. In some cases, these response functions may be directly derived from Eq. (1) and calculated without directly resolving the equations of motion.

- Then, an error function $E(\chi)$ or the root-mean-square difference between the measured functions and their corresponding modeling functions is calculated from:

$$E(\chi)=\sum_{i=1}^{N_R}\left[\sqrt{\frac{1}{N}\sum_{j=1}^{N_F}{W_{ij}}^2[F_{Mij}(\chi)-F_{Eij}]^2}\right] \quad (3)$$

where N_R is the number of the reference functions used in the calibration; N_F is the number of frequencies considered in the integration; F_{Mij} and F_{Eij} are the modelling and experimental values of the *i*th response function at the *j*th frequency, respectively; and W_{ij} is their relative weighting. The weighting is assigned based on the relative reliability of each reference function and the importance of each frequency, which are further discussed in Sections 4 and 5.

- The unknown parameters ($\chi=P_{u1}, P_{u2},\ldots, P_{ui},\ldots, P_{un}$) are varied within their constrained ranges until the resulting error function in Eq. (3) attains its minimum value. This is basically a mathematical optimization process. While many optimization methods and programs are available [9,33,34], the best choice may be model-specific, and it can be identified by testing each method using the numerical method described in Section 2.4. The goodness of the curve fitting is usually assessed using the *R*-value of the curve regression, the minimum error value, and/or the percent difference between the modeling and reference functions in the frequency range of interest.

2.2. The relationship between VT and DPR functions

A novel theorem of mechanical vibration was derived in our recent study [22], which describes the theoretical relationship among the frequency response functions of a mechanical system at its boundaries and inside the system. According to this theorem, the relationship between vibration transmissibility and apparent mass of a mechanical system can be generally expressed as follows:

$$\sum M(\omega)=\int T(\omega)\cdot \mathrm{d}m+\sum T_b(\omega)\cdot(c_b/\mathrm{j}\omega-k_b/\omega^2), \quad (4)$$

where M is the apparent mass in a direction; T is the motion transfer/transmissibility function in the same direction; m is the distributed mass throughout the system; subscript 'b' denotes the element or function at the boundary; and k_b and c_b are the boundary connecting stiffness and damping, respectively.

As examples, the specific relationships between the vibration transmissibility and apparent mass for each model shown in Fig. 2 are presented in Appendix A. These equations express that the total apparent mass in a specific direction is equal to the linear sum of the mass-weighted transmissibility functions distributed throughout the system in the same direction [22]. According to this theorem, the transmissibility function of each mass element (T_i) in

Eq. (4) is generally not that directly measured at a single point on or in the human body (T_{xyz}); instead, the transmissibility function is representative of the overall vibration of the substructure or tissue simulated as a lumped mass. Mathematically, the representative transmissibility of a substructure (S_i) with a mass (m_i) can be expressed as follows [22]:

$$T_{\mathrm{i}}=\frac{1}{m_{\mathrm{i}}}\int_{Si} T(x,y,z)\cdot \mathrm{d}m \quad (5)$$

2.3. Calibration methods

Mathematically, the series of mass values can also be considered as a function. Then, the theorem expressed in Eq. (4) defines the relationships among the following three types of functions: vibration transmissibility (VT), distributed mass (Mass), and interface/driving-point response functions (DPR). Using Eqs. (1) and (3), it can be proven that if two of the three function types are determined, the other function type can also be determined, which is further elaborated and demonstrated in Section 3. Interestingly, the three possible two-function combinations of the three function types correspond to the three typical calibration methods: VT method, DPR method, and combined VT and DPR method. In some special cases, the DPR method can be applied without the use of mass information [7–9]; this simplified method is termed as the DPR-alone method in the following presentation. Besides the mass information, the other distributed properties such as stiffness, Young's modulus and damping properties, can also be considered as part of the references or constraints in the model calibration if they can be reliably measured or estimated [11,12]. The methods using the combinations of VT, DPR, mass, and other property information are referred to as hybrid calibration methods in this study.

2.4. A numerical method for testing the calibration methods

Solution uniqueness is one of the essential criteria for validating the calibration for some models [35]. While solution uniqueness can be theoretically proven in some cases, it is difficult to analytically prove uniqueness in other cases, especially for models with nonlinear parameters. As an alternative approach, a numerical testing method has been proposed to check the uniqueness of the calibration solution [22]. Similar to the analytical approach, the reference functions are assumed to be accurate for the model to be calibrated. This bypasses any problems inherent with the measured reference functions so that the advantages and limitations of the calibration methods themselves can be clearly identified. The specific procedures of the calibration test implemented in the current study are outlined as follows [22]:

a. A set of reference parameters for a given model is assumed. For the purpose of the numerical testing, these parameters do not have to be accurate or validated. However, it is better to select the reference parameters based on the available information from previous studies or the preliminary values calibrated using available response functions. Examples of the parameter values for the models shown in Fig. 2 are listed in Table 1.

b. The equations of motion or Eq. (1) for each model with the assumed reference parameter values are written; the frequency response functions of the model in the frequency range of concern are calculated using the method described in Section 2.1; these functions are used as the accurate reference functions in the numerical test.

c. With the reference functions replacing the experimental data, the same procedures as outlined in Section 2.1 and the same computer program as designed to conduct the original calibration of the model are used in the numerical test [9,15]. Three numerical calibration trials are performed with randomly generated initial values of the parameters. Each initial parameter value is within the range of ± 15 percent from its reference value listed in Table 1. Each parameter is allowed to vary within the range of 0.5 – 1.5 times the reference value during the optimizing process of the calibration.

d. If each parameter value reliably converges to the reference value after a sufficient number of initial search cycles (one cycle is completed if every parameter is optimized once), independent of the initial conditions, the calibration method is considered acceptable for achieving a unique solution.

The existence of a theoretical unique solution does not guarantee a reliable solution in the practical calibration [22]. Besides testing uniqueness, the numerical method can also be used to explore the robustness and efficiency of the calibration methods and algorithms. For example, after a large number (e.g., > 200) of optimizing search cycles, if any parameter of a model remains largely different (e.g., > 20 percent) from its reference value, but every modeling response function is very close to its corresponding reference function (e.g, $r^2 >$ 0.999), the solution may be considered non-robust. Such a solution will be very sensitive to the perturbations of the reference functions or the initial conditions in the numerical calibration with the measured reference functions.

It should be noted that the robustness of the calibration depends not only on the calibration method but also on factors such as the model structure, the relative weightings among the reference functions, the frequency weighting of each response function, and the mathematical optimization strategy or computing algorithm used in the curve fittings. While it is beyond the scope of this study to address all these issues, this study considered the same models, the same optimization algorithm (MS Excel Solver), and the baseline weighting (defined in Section 4.3) for each function in the numerical tests, so that the calibration methods can be directly compared. The parameter search strategy used in this study is also the same as that used in our previous studies [9,15,31]: the model parameters are listed in a consistent order for each calibration method; they are varied one-by-one sequentially so that the sum of the root-mean-square differences between modeling and reference functions is minimized.

2.5. Basic criteria for model calibration

Based on the mathematical and physical principles of the model calibration dictated by Eqs. (1), (3)–(5) and the knowledge and experiences gathered from previous studies, the major

factors that may influence the reliability of the model calibration and their related criteria are proposed as follows:

1. **Model structure.** The structure should be suitable for the intended applications of the model. The structure should also allow the modeling response functions to fit the reference functions well. If the overall system responses and the distributed responses are both of concern in the model applications, the model structure should also provide reasonable simulations of the human body substructures of interest.
2. **Sufficiency of reference functions.** If the distributed responses are of interest in the model applications, the number of reference functions used in the calibration should be sufficient to achieve a unique solution of the model parameters, as the distributed dynamic properties of the human body must be unique. The solution should also exhibit as little sensitivity as possible to perturbations of the reference functions.
3. **Accuracy of reference functions and parameter constraints.** Each reference function should be measured as accurately as possible with an available technology; each parameter should be constrained within its realistic range according to the understanding of the parameter.
4. **Representativeness of reference functions.** If the distributed responses are of interest, each reference transmissibility function should be adequately representative of the overall vibration of the substructure simulated as a lumped or element mass in a model, as required by Eq. (5); at least, the reference transmissibility should be measured at a representative location of the substructure.
5. **Integrity of modeling equations, programs, and results:** The modeling equations and programs have no errors; the modeling results must satisfy the equation of the relationships among the mass, transmissibility, and driving-point response functions.
6. **Goodness of curve fitting:** More weighting should be assigned to more reliable references in the calibration; the total root-mean-square (rms) value of the curve-fitting errors for the DPR functions should be ≤ 5 percent in the major frequency range of concern if the model is used for engineering applications; the error in the transmissibility match should be as small as possible.
7. **Validity of model parameters and predicted responses.** For the parameters that can be associated with the properties of a specific part of the human body or segment, their calibrated values should be realistic or within the natural ranges for the subjects participating in experiments for the measurement of the reference functions. If the predicted responses are directly measurable, they should also be compared with the experimental data. The reasons for any large difference between the model responses and experimental data should be identified.

Theoretically, there are infinite model structures; it is not difficult to propose a comprehensive model that can meet the first criterion. It is, however, a formidable task to obtain sufficient, accurate, and representative reference functions to calibrate the model.

This indicates that the second, third, and fourth criteria become the major constraints for the further development of the mechanistic and effects models, which are elaborated and extensively discussed in Sections 3–5. To reduce the technical difficulties, the model should be as simple as possible as long as its objectives can be achieved. An in-depth understanding of these criteria may help make appropriate simplifications or improvements of the model structure, which is demonstrated and discussed in Sections 5.6 and 5.7. For the design and analysis of tools, seats, anti-vibration devices, and test apparatuses, it may not be necessary to use the transmissibility functions or to require a unique solution in the model calibration. For such applications, the second and fourth criteria are not required, which must also reduce the requirements of the model structure. To closely simulate the critical DPR functions required for such applications, the model structure can be selected or designed based on the characteristics of the DPR functions [35].

3. The sufficiency of reference functions

This section addresses the second criterion by identifying how many and which reference functions are necessary to achieve a unique solution of the parameters for each calibration method.

3.1. Vibration transmissibility (VT) method

The VT model calibration method utilizes combinations of VT functions and mass information [10,25]. According to Eq. (4), such combinations can uniquely determine the sum of the DPR functions; they should be sufficient to calibrate a model. This can be explicitly proven using Eq. (1) by assuming that the human body can be approximately simulated as a linear system. Specifically, the VT functions $(\mathbf{T}=\ddot{\mathbf{u}}/\ddot{u}_0)$ can be derived from Eq. (1) and expressed as follows:

$$\mathbf{T}=[\mathbf{M}+\mathbf{C}/\mathrm{j}\omega+\mathbf{K}/(\mathrm{j}\omega)^2]^{-1}[\mathbf{M_0}+\mathbf{C_0}/\mathrm{j}\omega+\mathbf{K_0}/(\mathrm{j}\omega)^2]\mathbf{I}_0, \quad (6)$$

where $\mathbf{I}_0$ is the driving-point identity vector with its elements either equal to 1 (driving point) or 0 (non-driving point). If the system parameters are changed proportionally or scaled by a common factor (λ), Eq. (6) remains unchanged because the scaling factor is canceled, which can be expressed as follows:

$$\mathbf{T}(\lambda\cdot\mathrm{parameters})=[\lambda\mathbf{M}+\lambda\mathbf{C}/\mathrm{j}\omega+\lambda\mathbf{K}/(\mathrm{j}\omega)^2]^{-1}[\lambda\mathbf{M_0}+\lambda\mathbf{C_0}/\mathrm{j}\omega+\lambda\mathbf{K_0}/(\mathrm{j}\omega)^2]\mathbf{I}_0=\mathbf{T}(\mathrm{parameters}) \quad (7)$$

This equation means that a given set of transmissibility functions can correspond to infinite sets of parameters; the transmissibility alone is not sufficient for uniquely determining the model parameters. However, the difference between any two sets of possible solutions is the scaling factor. This factor can be identified if the mass information of the system is known. This means that the model parameters can be determined uniquely if the mass information is provided. Hence, the transmissibility method requires both transmissibility and mass information of the system for the calibration.

This can also be further understood by examining an alternative expression of the VT functions. Because the proportional change does not affect the VT functions, each VT

function (T_i) in Eq. (6) must be a function of the linear ratios of the system parameters, which can be expressed as follows:

$$T_i = T_i\left(\frac{c_1}{m_1}, \frac{c_2}{m_1}, \ldots, \frac{c_n}{m_1}, \ldots, \frac{c_1}{m_2}, \frac{c_2}{m_2}, \ldots, \frac{c_n}{m_2}, \ldots, \frac{k_1}{m_1}, \frac{k_2}{m_1}, \ldots, \frac{k_n}{m_1}, \ldots, \frac{k_1}{m_2}, \frac{k_2}{m_2}, \ldots, \frac{k_n}{m_2}, \ldots\right) \quad (8)$$

If the VT functions are known, the ratios can be determined by solving Eq. (8) for each model. If the mass values are also given, the remaining parameters can be determined from the resolved ratios. For example, Eq.(8) for Model-(a) can be written as follows [34]:

$$T_1 = \sqrt{\frac{1+(2\xi\cdot\omega/\omega_n)^2}{(1-\omega^2/\omega_n^2)^2+(2\xi\cdot\omega/\omega_n)^2}}, \quad \omega_n = \sqrt{k_1/m_1}, \xi = c_1/(2m_1\omega_n) \quad (9)$$

If T_1 is given, its values at different frequencies (ω) can be used to write specific algebraic equations from Eq. (9) to find the valid solution of the parameter ratios (k_1/m_1 and c_1/m_1). If the m_1 value is known, the k_1 and c_1 values can be determined from the resolved ratios.

These theoretical predictions were verified using the numerical testing method. The models shown in Fig. 2 and the parameter values listed in Table 1 were used for the test. The numerical testing also revealed that, for some models, it is not necessary to require every mass value and/or transmissibility function within the model to obtain a unique solution. For example, only the transmissibility functions for m_3 and m_1 or m_2 of Model-(b) are necessary if all the mass values are given. If all the transmissibility functions and the total mass of the system are given, it is not necessary to require mass values for m_1 and m_2 in the calibration of this model. This is because at least a portion of the mass elements in the multi-body structure are physically connected to each other, and some of their motions are not independent. Mathematically, it is not necessary to require every VT function expressed in Eq. (8) to determine the parameter ratios nor every mass value to determine the stiffness and damping parameters from the ratios. This feature is useful for reducing the burden of the measurement of the reference transmissibility functions and mass values. However, if a model consists of more than one motion transmission path, a proportional variation could occur within each path without affecting the overall transmissibility in the system. This requires that adequate VT functions and mass information be provided for each path in the calibration. For example, the Model-(b) has two paths: m_{01}–m_3 path and m_{01}–m_1–m_2 path. Besides all the mass values, at least one transmissibility function is required for each of the two paths (e.g., for m_{01}–m_3 path: T_3; and for m_{01}–m_1–m_2 path: T_1 or T_2).

While the numerical testing method can be used to explore the minimum requirements or to check the sufficiency of the given reference functions for a specific model, the above analyses identify the general minimum requirements as follows:

i. If a model includes mass elements rigidly attached to the foundation in motion, these mass values must be provided or determined using other approaches. This is because the possible variations of these mass values do not affect their unity transmissibility.

ii. It is necessary to include at least one transmissibility function in each motion transmission path of a model in the frequency range of concern and at least one mass value in each path to achieve a unique solution of the calibration. Additional VT functions and/or mass values can increase the robustness of the solution.

The term 'motion transmission path' in the above requirements is a generalized concept; each series of structures in models with multiple series, each driving point in models with multiple driving points, or each vibration direction in models with multiple response directions is considered as a separate path. For example, Model-(b) has two paths because it has two series of independent substructures. Model-(f) also has two motion transmission paths because it has two driving points. Model-(c) has three paths because it has three vibration directions (vertical, rotational, and cross-axis). This concept is also applied when identifying the requirements for other calibration methods.

The geometric parameters (R_m and α) in Model-(c) define the location of the mass center of m_2; these parameters are nonlinear factors in the equations of motion. If the mass center is also known or estimated using a geometrical model, a robust calibration solution (the maximum error of the parameters < 1 percent after 30 search cycles) will be observed, similar to the applications of the transmissibility method for the other five models. Even if these nonlinear factors are included among the unknown parameters in the calibration, the numerical test trends toward a unique solution. This suggests that if appropriately applied, the transmissibility method can uniquely determine both linear and nonlinear parameters.

3.2. Driving-point response (DPR) method

The DPR calibration method generally uses combinations of DPR functions and the distributed mass information. If the mass values (m_i) for a system are known, Eq. (8) can be simplified as follows:

$$T_i = T(c_1, c_2, \ldots, c_n, k_1, k_2, \ldots, k_n, \ldots) \quad (10)$$

Substituting Eq. (10) into Eq. (4), the resulting equation can be generally expressed as follows:

$$\sum M = \sum m_i \cdot T_i(c_1, c_2, \ldots, c_n, k_1, k_2, \ldots, k_n, \ldots,) + \sum T_b(c_1, c_2, \ldots, c_n, k_1, k_2, \ldots, k_n, \ldots) \cdot (c_b/\mathrm{j}\omega - k_b/\omega^2) \quad (11)$$

If the precise DPR functions (M_i) for the system are given, the same number of algebraic equations as the number of the unknown parameters can be established by applying Eq. (11) to the same number of different frequencies, similar to what was done in Section 3.1. Unlike the linear algebra equations that can be written from Eq. (4) for the theoretical proof of the CTD method [22], the algebra equations written from Eq. (11) are nonlinear, and the solutions of the parameters are not unique if only one group of such equations is used in the solution. However, there is theoretically no limitation to consider as many groups of equations as necessary to identify the unique solution for each parameter. For example, two groups of equations for Model-(a) with frequencies of 4, 5, and 8 Hz can be written as follows:

$$\begin{cases} M(2\pi\cdot 4)=m_0+T_1(2\pi\cdot 4)\cdot m_1 \\ M(2\pi\cdot 8)=m_0+T_1(2\pi\cdot 8)\cdot m_1 \end{cases} \quad (12)$$

$$\begin{cases} M(2\pi\cdot 5)=m_0+T_1(2\pi\cdot 5)\cdot m_1 \\ M(2\pi\cdot 8)=m_0+T_1(2\pi\cdot 8)\cdot m_1 \end{cases} \quad (13)$$

The transmissibility magnitude (T_1) for this model is expressed in Eq. (9) and it is a function of the two unknown parameters (k_1 and c_1). These parameters can be resolved from each group of equations if the apparent mass function and the mass values are given. For demonstration purposes, the mass values in Table 1 and the apparent mass calculated from Eq. (1) for this model with the parameters in Table 1 were used to resolve the k_1 value. Two positive solutions for Eq.(12) are 44.115 kN/m and 285.375 kN/m, and solutions for Eq.(13) are 44.115 kN/m and 621.476 kN/m. Obviously, the two groups of solutions include one identical value (k_1=44.115 kN/m), which is also identical to the reference value listed in Table 1. This is because this value is valid for the given mass and DPR function at any frequency. The other solution varies by frequency. Therefore, there is only one valid solution. These processes are generally applicable to any other models. They theoretically demonstrate that the combination of the DPR functions and the mass information can uniquely calibrate a model. This theoretical prediction was also verified using the numerical testing method for all the models shown in Fig. 2.

Eqs. (8) and (11) reveal that the difficulty of the calibration solution generally increases with the number of unknown parameters. It should also be noted that the solutions using these equations are only for the mathematical proof of the calibration methods. This solution method should not be applied to conduct actual calibrations using measured reference functions because the theoretical solution requires precise reference functions. An approximation method has to be used to deal with the imperfections among the reference functions. The curve fitting method based on the criterion of the least root-mean-square error seems to be a reasonable choice for practical calibrations. The numerical testing method applied in the current study also uses this tactic.

Different from the VT function, each DPR function includes both motion and mass information, as revealed in Eq. (4). Hence, the DPR functions alone are adequate to determine the parameters of some simple models. This can also be proven using the relationship theorem. For example, if the apparent mass (M) for Model-(a) is known, Eq. (A1) can be used to estimate the mass elements and the transmissibility function as follows:

$$m_0=\underset{\omega\to\infty}{M}, m_1=\underset{\omega\to 0}{M}-m_0, T_1=\frac{M-m_0}{m_1} \quad (14)$$

Once these functions are determined, the remaining stiffness and damping values of this model can be uniquely determined, according to the transmissibility method described in Section 3.1. The numerical test confirms these analytical predictions. Numerical testing also reveals that it is not necessary to consider very high or very low frequencies required in Eq.

(14) to achieve an accurate solution; the solution is very robust and efficient if the frequency range of the DPR function adequately covers the entire resonant frequency range.

The DPR magnitude alone and phase angle alone have also been used to calibrate some models [8,36]. While the magnitude-alone method is acceptable, the phase angle-alone method is not adequate. This can be proven using the relationship theorem [22]. Specifically, if each parameter of a model is multiplied by λ and Eq. (6) is used, the relationship theorem expressed in Eq. (4) can be generally expressed as follows:

$$\sum M(\lambda)=\int T(\lambda)\cdot d(\lambda m)+\sum T_{\mathrm{b}}(\lambda)\cdot(\lambda c_b/\mathrm{j}\omega-\lambda k_b/\omega^2)=\lambda\int T\cdot d(m)+\lambda\sum T_b\cdot(c_b/\mathrm{j}\omega-k_b/\omega^2)=\lambda\sum M \quad (15)$$

This equation indicates that the proportional change of the parameters also proportionally changes the magnitudes of the DPR functions, but the change does not affect the phase angles. This means that the phase angle alone, similar to the transmissibility alone, is not adequate to uniquely calibrate the model. However, if the distributed mass is also provided, together with the phase angle, the calibration solution can be unique if the corresponding magnitude alone can result in a unique solution.

Similar to Model-(a), Model-(d) shown in Fig. 2 can also be uniquely and robustly calibrated using the DPR-alone method. If the two DPR functions for Model-(e) are provided, they can also be used to uniquely and robustly calibrate this model. Although Model-(f) has three effective dofs (the dofs excluding the unsuspended mass elements), two DPR functions are also sufficient to uniquely calibrate this model. This is because the three resonances (8, 35, and 235 Hz) are clearly differentiable from the two impedance values ($Z_{\mathrm{Fingers}}=\mathrm{j}\omega M_{\mathrm{Fingers}}$ and $Z_{\mathrm{Palm}}=\mathrm{j}\omega M_{\mathrm{Palm}}$), and the DPR functions provide the information regarding the response distribution, as shown in Fig. 3. The total hand impedance (the sum of the finger and palm impedances) was measured in many studies. Although the total impedance may also include all the resonance information [17,36], it does not provide sufficient distribution information. As a result, the total impedance alone is not adequate to uniquely calibrate Model-(e) or Model-(f) [36]. In such cases, it is necessary to provide additional mass distribution information to achieve a unique calibration. If it is difficult to directly determine the distributed mass values, the known or estimated ratios among the mass values (e.g., $m_{01}/m_{02}\approx$ ½ [9]) may also be used in the calibration [36].

Model-(c) also has three dofs and two DPR functions (the apparent mass in the *z* direction and the cross-axis apparent mass in the *x* direction) [7]. Because the human body is a heavily damped system, there is only one clear resonance for each DPR function, as shown in Fig. 4. The DPR-alone method cannot achieve a unique solution for such a model because the two translational DPR functions can only control the model properties in the two translational paths (vertical and cross-axis directions) but they cannot control the model properties in the rotational direction (the third motion transmission path). In other words, although the cross-axis response (M_{x-z}) results from the rotational vibration of m_2, the same response can result from different combinations of the rotational parameters. This is shown in the three groups of the parameter values listed in Table 2, which were identified from the numerical testing of this model. Probably for this reason and the small unsuspended mass in the fore-and-aft

direction, m_1 was taken as zero in the reported study [7]. This, however, does not eliminate the major uncertainty which primarily results from the rotational response. The numerical testing results listed in Table 2 also indicate that there are certain relationships among the rotational parameters for the given translational DPR functions; this indicates that if one of the rotational parameters is fixed, the others can also be determined. In other words, if the DPR functions and the mass center (R_m) or inertial moment (J) are given, the DPR method can uniquely calibrate the model, as also verified in this study.

Although the structure of Model-(b) is simpler than Model-(c) or Model-(f), it is impossible to use the DPR-alone method to uniquely calibrate this model. This is primarily because Model-(b) has only one driving point; the single DPR function cannot provide the distribution information for the two paths. The single DPR resonance also makes it very difficult to differentiate the three resonances of this model. While the unsuspended mass (m_{01}) and the total mass of the system can be identified from the single DPR function, at least two other mass elements (e.g., m_1 and m_3) are needed in order for the DPR method to uniquely calibrate this 3-dof model. These predictions were verified using the numerical test. The testing results also suggest that the solution may not be robust.

Based on these analyses and numerical tests, the general requirements for the DPR method are proposed as follows:

- **i.** If the number of DPR functions is less than the number of the motion transmission paths in the model, the DPR-alone method cannot uniquely calibrate the model but it can determine a portion of the model parameters; the specific parameters depend on the model structure and the information provided by the DPR functions.
- **ii.** If both real and imaginary parts of the DPR functions at all driving points/paths of a model are provided, and if the number of major resonances clearly differentiable in the DPR functions is not less than the number of effective dofs (the dofs excluding the unsuspended mass elements) in the model, the DPR-alone method can be used to obtain a unique solution for the model calibration.
- **iii.** The combination of the DPR functions at all the driving points and sufficient number of mass information can uniquely calibrate a model; the required minimum mass information depends on the model structure.

3.3. Combined transmissibility and driving-point response (CTD) method

The CTD calibration method utilizes combinations of DPR and VT functions [6,26,27]. Using Eq. (4), our previous study has proved that the mass values and boundary stiffness and damping values can be uniquely determined if all the DPR functions at all driving points and the vibration transmissibility functions for all the mass elements of a model are provided [22]. Then, the remaining model parameters can be uniquely determined according to the theoretical proof described in Sections 3.1 or 3.2. The reported study also further demonstrated that it is not necessary to require every VT function, because the DPR functions include some VT information, as also demonstrated in Section 3.2. An effective approach to determine the required minimum number of VT functions is to use the DPR method to identify the sources of uncertainty and to use the corresponding VT function(s) to

supply the missing information. For example, as above-mentioned, the major source of uncertainty for Model-(c) is associated with the rotational degree-of-freedom. Hence, if the cross-angle transmissibility ($T_{\theta-z0}=\theta/Z_0$) is available, the rotational parameters can be uniquely calibrated using their relationships with their values (J_{DPR}, $k_{2\mathrm{DPR}}$, $c_{2\mathrm{DPR}}$, R_{DPR}) identified using the DPR-alone method. Specifically, the relationships can be written as follows:

$$J=\beta\cdot J_{\mathrm{DPR}}, k_2=\beta\cdot k_{2\mathrm{DPR}}, c_2=\beta\cdot c_{2\mathrm{DPR}}, R=\sqrt{\beta}\cdot R_{\mathrm{DPR}} \quad (16)$$

where β is a scaling factor. With these relationship equations, these rotational parameters can be calibrated by minimizing the differences between the modeled and measured cross-angle transmissibility functions by optimizing the β value without changing any other calibrated parameter using the DPR-alone method.

If the distributed mass information for Model-(c) is not available, it is also necessary to use the VT functions to provide the distribution information. The numerical test results suggest that in order to meet the minimum conditions, the VT functions for m_3 and either m_1 or m_2 are required. If only the total DPR function is used in the calibration of Model-(f), the VT functions for m_1 and either m2 or m3 are required. If the VT function and mass value of m_3 for Model-(f) are provided, together with the two DPR functions, the calibration solution for this model can be very robust.

This study also confirmed that the CTD method is not robust in some cases, especially for models with multiple motion transmission paths such as Model-(b) and Model-(f). This is partially because the VT functions are not sensitive to the variations of the model parameters due to the large damping properties of the human body and the near-unity transmissibility featured at frequencies below the fundamental resonant frequency, as shown in Fig. 5. For example, according to Eq.(A2), it is very difficult to determine the mass values if the T_1, T_2, and T_3 values are close to 1.0 or are not sensitive to the parameter variations. In other words, the model parameters will be very sensitive to the perturbations of the measured VT functions in such conditions. The difficulty obtaining a reliable solution is also partially because the VT functions at some different locations or substructures are similar across a large frequency range [22], as also shown in Fig. 5. Furthermore, the independent proportional variation of the parameter values in each motion transmission path of a multiple-path model does not change the VT functions, as expressed in Eq. (6). The total DPR function can remain more or less the same with different distributions of the mass properties among the motion transmission paths, as indicated in Table 3, which provides three alternative numerical testing solutions for calibrating Model-(b). Such a solution may also reflect a distinctly local optimization, which may make it difficult to find a globally-optimized solution using a conventional optimization algorithm. While a rigorous optimization method may be considered [33,34], this study proposes a special tactic to deal with such situations. First, the local optimization is obtained using the conventional algorithm. Then, while the parameters in each motion transmission path are kept at the same relationships, the property distribution ratios among the motion transmission paths are varied to minimize the errors of the curve fittings. As demonstrated by the results presented in Table 3, this can eventually lead to a globally optimized solution.

Based on the above analyses and numerical test results, the critical requirements of the CTD method are identified as follows:

- **i.** Besides the total DPR function and the information for the unsuspended mass at each driving point, at least one VT function for each motion transmission path of a model structure is required to uniquely calibrate the model.
- **ii.** If the DPR at each driving point in each direction is given, the requirement for the unsuspended mass information is eliminated; the minimum number of VT functions can also be reduced or eliminated, depending on the specific model structure.

In addition, some special tactics may be required to calibrate the models with multiple motion transmission paths to achieve the global optimization of the solution. To reduce the undesired effects of the similar VT values at low frequencies and their insensitivity to the parameter variations, it may also be a good tactic to use more VT values or weight of the VT functions in the resonant frequency range and at higher frequencies in the calibration to increase the robustness of the solution. However, the VT values at high frequencies may be below the noise level and such data should also be avoided.

4. The accuracy and representativeness of reference functions

This section discusses the issues related to the third and fourth criteria presented in Section 2.5. In reality, no model structure can fully represent the human body; every measured reference function includes some errors. It is also impossible to synthesize a VT function that provides an exact representation of the overall vibration of a substructure. For these reasons, no modeling response function can precisely match the measured reference data. While further studies are required to improve the technologies and methods for measuring and/or synthesizing the reference functions, this section discusses the effects of the reference uncertainties in the calibration and the methods for reducing those undesired effects.

4.1. Relative reliabilities of the reference functions

The degree of uncertainty varies with each specific reference function. The total mass of the human body can be accurately measured. The mass of a substructure can also be estimated from its geometry or volume and the mass densities of the tissues. Similarly, the distributed mass elements in a finite element model can be reasonably determined without any major difficulty. However, it can be challenging to accurately determine the mass of some substructures modeled as lumped elements in some models. For example, it is very difficult to determine the unsuspended mass in a lumped parameter model using any method without using any DPR function. Accurately determining the effective mass of the shoulder or trunk involved in the response to hand-transmitted vibration is also quite challenging. It is also very difficult to accurately determine how much mass corresponds to a VT function measured at a specific location on the head. While the measurement of DPR functions has improved in recent years [37], it remains challenging to accurately measure VT functions on some substructures, especially using conventional accelerometers. The VT functions on the human body may also be spatial [38]. Also importantly, it is currently not practical to measure the internal transmissibility inside the body of a living subjects using in-vivo

technologies. These obstacles, together with complications in identifying the exact boundaries of substructures, make it difficult to synthesize representative VT functions for calibrating lumped-parameter models. These observations suggest that DPR functions are generally more reliable than VT functions, which is consistent with the observations made in a reported study [39]. Naturally, it is a good strategy to avoid using less reliable reference functions as much as possible in model calibrations.

4.2. The effects of reference inconsistencies

Eq.(4) indicates that the combinations of reference functions used in the calibration methods are likely to include overlapping information, especially when redundant functions for some substructures are used in the calibration. This may produce the proverbial double-edge sword; while additional reference functions can increase the robustness of the calibration, the added information may also reduce the reliability of the model if the functions fail to provide information consistent with the system properties. In such cases, it is impossible to generate suitable matches among the modeling and measured functions. Compromises have to be made in the calibration solution, as observed in a reported study [24]. If the DPR functions are more reliable than the VT functions, the CTD method may be used to calibrate only those parameters that cannot be uniquely calibrated using the DPR method. Alternatively, the relative weighting of the VT functions can be reduced in the calibration.

4.3. Baseline weighting

Besides dealing with the different reliabilities of the measured reference functions, function weighting is also required to deal with the different units or scales of the functions. While inconsistent weightings were used in the past, a baseline weighting should be established to guide the application of the appropriate weighting for further studies. The relationship theorem provides the natural baseline weightings among the response functions. As illustrated in Eqs. (A1 – A6), if the baseline weightings for the real and imaginary parts of the apparent mass are taken as 1.0, the equivalent baseline weighting for each VT function (W_{Ti}) is its corresponding mass value (m_i) or

$$W_{Ti}=m_i \quad (17)$$

Because the magnitude of the mechanical impedance is equal to $M \cdot \omega$, the corresponding baseline weighting in the calibration using the impedance is that in Eq. (17) multiplied by ω. This relationship also indicates that the impedance method weights the high frequency components more than the apparent mass method.

5. Evaluations, interpretations, and improvements of the model calibration

The development of human vibration models is usually an iterative process. The examination and improvement of the calibrated models may be performed at any stage of the development. While it is beyond the scope of this study to address all the aspects of model validation according to the proposed criteria, some examples are introduced in this section to demonstrate the applications of the above-presented theories and methods to evaluate, interpret, and improve the model calibration.

5.1. Check the integrity of the modeling equations, computing programs, and results

Criterion 5 emphasizes a good common practice: to carefully check the modeling equations and programs but not to artificially revise the modeling results to match the experimental data. The novel theorem expressed in Eq. (4) provides a new approach to examine the integrity of the modeling equations, programs, and results. Specifically, if the equations of motion for a model contain some errors, or the modeling program includes bugs, or the results are modified for any reason, the modeling response functions may not satisfy the relationship theorem or Eq. (4). For example, the modeling response functions calculated using the equations of motion for the 6-dof model reported in [24] do not satisfy Eq. (4). This led to the identification of errors in the reported stiffness and damping matrices. It should also be noted that the satisfaction of Eq. (4) is a necessary condition, but this condition alone is not adequate for assuring model integrity. Some other methods should also be considered in the examination.

5.2. Check the sufficiency of the number of reference functions and the suitability of parameter constraints

The requirements presented in Section 3 can be used to conduct a quick check of reference sufficiency for many models. For example, the hand-arm system model reported in [24] has six dofs (four translational dofs and two rotational dofs), which includes the hand structure similar to that of Model-(f) shown in Fig. 1. However, only one DPR function for the entire hand-arm system was measured and used in the calibration. Four translational VT functions were respectively measured on the surfaces of the wrist, forearm, elbow, and upper arm, which were used to synthesize three VT functions for the calibration. The three VT functions theoretically provide redundant translational vibration information, but they cannot provide adequate rotational vibration information for the two rotational dofs. Definite values of the mass parameters were not provided. Those mass values, together with the stiffness and damping parameters, were considered as variables in the calibration. According to the sufficiency requirements presented in Section 3, the provided reference functions are not adequate for any of the three calibration methods used in that study to achieve a unique solution of the model parameters. Consequently, each parameter can take different values within the range of its constraints, depending primarily on the calibration method, error tolerance of the calibration, reference function weighting, and optimization algorithm. If the constraints are not appropriately defined, there could be substantial differences among the models calibrated using different methods. More importantly, some of the calibrated parameters may not be realistic. For example, the total mass of the fingers calibrated using the VT method was only 22 g, which was only 17 percent of that (130 g) calibrated using the DPR method in the same study [24]. These observations partially explain why the models calibrated using the three methods were substantially different in that study.

5.3. Check for accuracy and representativeness of the reference functions

Except for the low-frequency apparent mass which should be close to the seated whole-body mass measured without vibration exposure, it is difficult to directly judge the general accuracy and representativeness of the measured response functions. This partially explains why the reported experimental data were very different [36,40]. The modeling can be used

as an indirect method to help diagnose some of the possible problems. For example, because the DPR-alone method can reliably estimate the unsuspended mass, it can be used to check whether the tare mass is correctly subtracted from the measured data.

Fig. 6 shows the comparisons of some experimental data and modeling results reported in a recent study [15]. In that study, the DPR-alone method was used to calibrate Model-(f) shown in Fig. 2 using the impedance values measured at the fingers and palm of the hand. This method forces the modeling impedance values to match the experimental data, but it does not apply any control to the VT functions. The predicted VT functions for m2 and m3 agree very well with the experimental data measured at the wrist and upper arm, respectively. These observations suggest that the model structure is acceptable for simulating the system, and these measured VT functions are acceptable for approximating the overall motions of their corresponding substructures with the postures used in the experiment [15,37].

The reference functions were not well correlated in another study [24]. The CTD method was claimed to be the best among the three calibration methods used in that study, which should force matches for not only the impedances but also the VT functions. However, substantial differences are observed in the comparisons of both VT and DPR functions, as shown in Fig. 7. Besides the differences between the modeling and measured resonant frequencies, the modeling impedance is about 28 percent (on average) less than the measured data, as shown in Fig. 7(b). According to Eqs. (7) and (15), proportionally increasing the original model parameters by 28 percent does not change the ‘goodness’ of the fits for the VT functions, but it can greatly improve the matches for impedance, as also shown in Fig. 7(b). This increase, however, would further inflate the already overestimated hand mass from 630 g (34 percent larger than the normal hand mass, 469 g) to 806 g. Hence, it is impossible for the modeling functions to match with the measured data well within the natural ranges of the system properties. This is an indication of substantial inaccuracies and/or improper representations among the measured functions. This is further confirmed from the following observations: the wrist is not part of the palm-hand dorsum substructures, but the VT function measured at the wrist was used to represent the motion on those substructures; similarly, the vibration of the shoulder was not measured, but that measured on the upper arm was used to represent the response of the shoulder [24]. With such mismatches, it is impossible for the CTD method to create a valid model for predicting the distributed biodynamic responses. These inconsistencies also further explain why the model parameter values calibrated using the three methods were largely different in that study.

It should be emphasized that good matches between the modeling and measured data are a necessary but not sufficient condition for assessing the quality of the measured data. Theoretically, one can always get the modeling responses to match well with any measured data by selecting a special model or increasing the model structural elements if the second and fourth criteria (sufficiency of reference functions and unique solution of model parameters) are not required in the calibration of some models. Such models should not be used to evaluate the reference functions.

5.4. Check the comparability of VT functions

Even if the VT functions are accurately measured, it may not be appropriate to directly apply them to validate a model in some cases. As shown Fig. 8, the finger VT function of the total vibration (vector sum of the three axis vibrations) measured on the dorsal surfaces of the fingers using a 3-D laser vibrometer is significantly larger than that predicted using Model-(f) calibrated using the DPR-alone method [15,41]. The major differences are likely because the measured VT function is not representative of the overall motion of the fingers simulated as a lumped mass in the model for the following reasons. First, the fingers can be virtually considered as layers of visco-elastic materials attached to the vibrating handle. In the major resonant range of the fingers, the transmissibility on the top surface of the materials generally reaches the highest transmissibility while the materials close to the contact surface remain near unity transmissibility. As a result, the overall transmissibility that can be synthesized using Eq. (5) is smaller than the transmissibility measured at the dorsal surface of the fingers. Second, the fingers are likely to have some rotational responses. They can cause some additional translational vibrations in the tangential directions on the dorsal surfaces of fingers, especially in pure shear or along the handle axial (y) direction. This may explain why the differences between the modeling and measured data are generally larger in the y direction than those in the other directions [15]. Furthermore, the measurement was carried out at limited locations on the index and middle fingers. The measured data may not adequately represent the overall vibration of all the fingers. For these reasons, the finger VT functions calculated from the DPR-calibrated models are not directly comparable with those measured on the dorsal surfaces of the fingers. This, however, does not mean that the model is invalid for predicting the overall translational vibrations of the fingers. On the other hand, if the CTD method was used to force matches between the transmissibility values, the calibrated Model-(e) or Model-(f) would certainly be invalid. Because it is very difficult to synthesize the representative transmissibility function of the fingers required by the VT and CTD methods, the DPR method seems to be the best option for calibrating the lumped finger model.

5.5. Check the values and characteristics of the predicted biodynamic properties

The apparent mass generally increases with body mass, but that correlation does not hold true for phase angle or transmissibility [1,2,7,27]. This is consistent with the implications of Eqs. (6) and (14). These phenomena suggest that the overall biodynamic properties of the human body vary near-proportionally with the body mass in the general population. This further explains why the major resonances of the whole-body vibration in the vertical direction generally fall within fairly narrow frequency ranges (3–6 Hz) [1,7,8,27]. These characteristics justify the normalization of DPR magnitudes with respect to body mass [1,2,27].

The characteristics of the human biodynamic properties may also be used to check the validity of the calibrated models or to help estimate some model parameters. Using a reported study as an example, the effective mass of Subject 12 is 87 kg, which is 1.4 times the median mass (62 kg); however, the inertial moment (9.41 kg m^2) of this subject was 52 times the median value (0.18 kg m^2) [7]. This is obviously incompatible with typically-observed proportions. As identified in Section 3.2, this is because the rotational parameters

were not controlled in the calibration, and they could take any random value. To eliminate the random variation, a constraint related to the body mass can be applied to the calibration. While the mass in a local structure generally increases with the total body mass, the rotational properties (J, k_2, c_2, and R_m) should also increase with the total mass. As a crude approximation, the relationship among subjects can be derived from the dimensional analysis of the inertial moment unit (kg m^2). For the derivation, this study made the following assumptions: (i) the mass density remains unchanged for different subjects; (ii) the mass varies proportionally with the volume of the body; and (iii) the volume is proportional to $(R_m)^3$. The derived relationship is expressed as follows:

$$J_S = \left(\frac{M_S}{M_{\text{Ref}}}\right)^{5/3} \cdot J_{\text{Ref}}, \quad (18)$$

where J_{ref} is the known reference value, J_S is the estimated value for a subject, M_S and M_{ref} are the mass values for the subject (S) and the reference subject (Ref), respectively.

For demonstration purposes, we can tentatively assume that the reported median values are correct and use them as reference values: J_{ref}=0.18 kg m^2 and M_{ref}=62 kg. Then, the J_{12} value for Subject 12 (M_{12}=87 kg) can be estimated from Eq. (17). It is approximately 0.32 (kg m^2), instead of 9.41 (kg m^2) that was reported before [7]. Using the revised J_{12} value, the β value in Eq. (16) can be determined. Then, the other rotational parameters can also be estimated from the β value. Similar revisions may also be applied to the rotational parameters for other subjects in the reported study [7].

5.6. Check the model structures

The knowledge generated from the current study may also be used to help improve the model structure design. Using Model-(c) as an example, the unsuspended mass in the fore-aft (x) direction is naturally very small, and m_1 can be taken as zero for simplifying its calibration [7]. However, this introduces another issue: the unsuspended mass in the z direction should not be ignored, as evidenced from the obvious differences between the modeling and the measured apparent masses at frequencies above 7 Hz shown in the reported study [7]. Such differences are likely to become more obvious if the frequency range is extended to frequencies above 10 Hz. Physically, the soft tissues between a vibrating surface and the bony substructures of the human body can be conceptually considered as a coiled spring with mass and damping properties distributed along the length of the spring. The mass in contact with the surface must move with the surface or vibrating foundation; therefore, a part of the spring mass can be simulated as an unsuspended mass in a lumped-parameter model of the whole body system. This can also be mathematically proved using the spring model. This may explain why the models with an unsuspended mass can usually provide a better fit to the measured responses than those without it and that the vast majority of the whole-body models include the unsuspended mass [2,8,27]. Similar phenomena have also been observed in the simulation of the hand-arm system responses [9,15,31]. Based on these observations, the original model can be improved by adding an unsuspended mass (m_0) to Model-(c) and the revised model is shown in Fig. 9. According to the above-presented analyses and numerical tests, the added mass will not increase the

difficulty of the calibration, but it is likely to increase the quality of the calibration. This improvement, together with the estimation of the rotational parameters described in Section 5.5, may make the model more meaningful. Furthermore, as reflected in Eq. (A3) in Appendix A and in the equations of motion of Model-c in the reported study [7], m_1 and m_3 in the model have the same horizontal vibration. This is not reflected in the model structure of the reported study, as shown in Fig. 2(c). This was corrected in the current study, and the proposed correction to the illustration is also shown in Fig. 9.

The improved knowledge of model calibration can also be used to help appropriately simplify the model structure. As shown in Fig. 2(f), the palm – wrist – forearm substructures along the forearm direction were modeled as a lumped element [9,15,31]. Some researchers criticized that this model could not predict the distributed dynamic responses, particularly at the wrist; hence, they modeled the palm as a separate mass element [24]. This criticism ignores the fact that the vibration power absorption measured at the palm along the forearm direction can be used as an approximate measure of the wrist joint vibration exposure [15,31,42]. It also ignores the fact that the dynamic force at the palm is highly correlated with that at the wrist joint in the major resonant frequency range of the hand – arm system, as can be demonstrated via the correlation (R^2=0.99) between the dynamic force derived from the impedance measured at the palm and the wrist acceleration derived from the transmissibility data measured at the wrist shown in Fig. 6. Also because the palm and wrist biodynamic responses are correlated with frequency-weighted acceleration [41–43], wrist injuries are likely to be associated with the weighted acceleration [44]. Furthermore, the wrist joint is much more rigid than the palm tissues along the forearm direction; the palm tissues basically serve as a cushion for the wrist joint in this direction. Hence, it is not necessary to consider the palm as a separate mass element in this direction, especially in the major resonant frequency range. While the separation is unlikely to increase the value of the model, it certainly increases the difficulty of the model calibration, as the increased dof requires more calibration references. Because such reference values were not provided, the increased complexity of the model structure led to low quality of the model calibration, as observed in the reported study [24].

Our previous study revealed that the DPR method may determine the role of each structural component of a model according to the characteristics of the given DPR references. In that study, the same model structure as that of Model-f shown in Fig. 2 was used to simulate the responses of the human hand-arm system in each of the three orthogonal directions (x, y, z). However, the calibrated parameter values showed that the palm and hand dorsum were ‘considered’ by the DPR method itself as separate entities for the x and y direction but the palm – dorsum – wrist – forearm was kept as one entity for the z direction [15]. This is because the given DPR references include the information that the wrist stiffness along the forearm or z direction is very large. As a result, it is not necessary to consider the hand dorsum and forearm as separated mass element in the lumped-parameter model. However, their equivalent connection stiffness in the x or y direction is small and they cannot be considered as one lumped mass because the wrist has a large rotational freedom in the x and y directions. This demonstrates that the exact assignments of the substructures in the human vibration modeling using the inverse dynamic approach may not be fully predetermined by a

researcher, but they may be interpreted or recognized from the results of the model calibration [9,15]. This feature further suggests that model calibration may be used a tool to explore the motion mechanisms of the human body or segments.

5.7. The interpretation of the fixed boundary in hand-arm system models

The hand – arm vibration models usually include a fixed boundary, as shown in Fig. 2. Some researchers interpreted the fixed boundary as a fixed substructure, e.g., the boundary in Model-(f) as a fixed shoulder [24]. Based on this interpretation, they criticized that Model-(f) ignored the coupled responses of the shoulder and other upper body substructures. The interpretation and criticism are invalid if the model parameters are determined using a calibration method. Because the shoulder of any human subject is not fixed in any experiment, the coupled responses must be reflected in the measured reference functions, especially the DRP function measured at the palm of the hand. Consequently, the model calibrated using the reference functions must reflect the equivalent mass, stiffness, and damping properties of the coupled substructures. For example, m_3 in Model-(f) actually represents the equivalent mass of not only the upper arm but also the shoulder and some other substructures [9,31]. The connections between m3 and the boundary (k_5 and c_5) represent the equivalent stiffness and damping properties of the upper arm, shoulder, and other upper body substructures. The fixed boundary in the model does not mean that there is an actual boundary in the real system. The boundary is a technical treatment of the substructure method for simplifying the model, which is widely used in the analyses of continuous engineering structures such as railway tracks and long bridges [34,45]. Of course, if the specific responses of the upper arm, shoulder, chest, neck, and head are of concern, they should be considered as separate components in the model. Otherwise, it is not worth increasing the complexity of the model structure and the difficulty of the model calibration. A model with more dofs is not necessarily better than a simpler model, especially if the complex model is not reliably calibrated using sufficient, accurate, and representative reference functions.

6. Conclusions

Based on a novel theorem and general knowledge of mechanical vibration, this study enhanced the understanding of the mathematical and physical principles of the model calibration using frequency response functions. Building upon this enhanced understanding, a set of criteria was proposed to guide the development of human vibration models. Guided by these criteria, this study systematically examined the three typical calibration methods. Besides theoretical analyses, a novel numerical testing method was also used in the examination. Using the theoretical analyses and numerical tests, this study identified the basic requirements of each calibration method for obtaining unique solution of the model parameters. While the proposed theories, methods, criteria, and requirements may serve as general guidance or tools for the further development of human vibration models, it is recommended to apply the numerical testing method to verify the selected calibration method before conducting any actual calibration.

This study demonstrated that all three methods can result in the same unique solution for a given model structure if all the requirements of each method are met in the model

calibration. However, the theoretical uniqueness does not guarantee the practical applicability of the calibration methods, depending on the model structure and the features of the given reference functions. Specifically, if the given reference functions do not adequately cover the frequency ranges of all important resonances, the calibration solution may not be unique or robust (efficient and/or insensitive to perturbation of references). Likewise, the calibration solution may lack robustness if the model includes multiple motion transmission paths, the given transmissibility functions are similar across a large frequency range, and/or the resonances are in similar frequency ranges. In general, if more reference functions are provided, the solution becomes more robust. Practically, however, as additional reference functions are used, more inconsistencies can arise among the reference functions for representing the biodynamic properties of the human body. This is because the measured functions may include errors and some of the transmissibility functions may not be adequately representative of the overall motions of the substructures simulated as lumped mass elements in the model. Because it is difficult to accurately measure and reliably synthesize a representative transmissibility, it is recommended to use it to calibrate only those components that cannot be uniquely calibrated using the other reference functions such as mass and driving-point response functions. Alternatively, less weighting can be applied to the transmissibility in the calibration. The proposed baseline weighting scheme can be used to establish benchmarks for weighting assignments. If the distributed responses in the human body or body segments are not of interest in the applications of the models to design and analyze tools, seats, anti-vibration devices, and testing apparatuses, it is not necessary to require a close simulation of the human body structure; it is neither necessary to use any transmissibility function nor to require a unique solution of the model calibration. This is because the interactions between the human body and the seat or tool are of major concern in such applications. Theoretically, the effect of the human body on the interactions can be largely represented by the driving-point response functions of the body. Therefore, the most important factor for such applications is to ensure the reliability of the apparent mass or mechanical impedance measured in a close simulation of real working conditions and the goodness of the curve fitting in the model calibration. For such engineering applications, it is recommended to control the average curve fitting error in the major frequency range of concern to within ± 5 percent.

Appendix A

The relationships between apparent mass and transmissibility in the example models Eq. (4) for the example models shown in Fig. 2 can be written as follows:

For Model-(a),

$$M(\omega)=m_{01}+T_1(\omega)\cdot m_1 \quad \text{(A1)}$$

For Model-(b),

$$M(\omega)=m_{01}+T_1(\omega)\cdot m_1+T_2(\omega)\cdot m_2+T_3(\omega)\cdot m_3 \quad \text{(A2)}$$

For Model-(c),

$$\begin{cases} M_z(\omega)=m_1+T_{2z}(\omega)\cdot m_2+T_{3z}(\omega)\cdot m_3 \\ M_{x-z}(\omega)=T_{1,x-z}(\omega)\cdot m_1+T_{2,x-z}(\omega)\cdot m_2+T_{1,x-z}(\omega)\cdot m_3 \end{cases} \quad \text{(A3)}$$

For Model-(d),

$$M(\omega)=m_{01}+T_1(\omega)\cdot m_1+T_1(\omega)\cdot(c_2/\mathrm{j}\omega-k_2/\omega^2) \quad \text{(A4)}$$

For Model-(e),

$$M_{\mathrm{Fingers}}(\omega)+M_{\mathrm{palm}}(\omega)=m_{01}+m_{02}+T_1(\omega)\cdot m_1+T_2(\omega)\cdot m_2+T_2(\omega)\cdot(c_4/\mathrm{j}\omega-k_4/\omega^2) \quad \text{(A5)}$$

For Model-(f),

$$M_{\mathrm{Fingers}}(\omega)+M_{\mathrm{palm}}(\omega)=m_{01}+m_{02}+T_1(\omega)\cdot m_1+T_2(\omega)\cdot m_2+T_3(\omega)\cdot m_3+T_3(\omega)\cdot(c_5/\mathrm{j}\omega-k_5/\omega^2) \quad \text{(A6)}$$

References

1. Griffin, MJ. Handbook of Human Vibration. London: Academic Press; 1990.
2. International Organization for Standardization, ISO-5982, mechanical vibration and shock – range of idealized values to characterize seated-body biodynamic response under vertical vibration. 2001
3. International Organization for Standardization, ISO-10068, mechanical vibration and shock – mechanical impedance of the human hand–arm system at the driving point. 2013
4. International Organization for Standardization, ISO-2631-5, mechanical vibration and shock – evaluation of human exposure to whole-body vibration – part 5: method for evaluation of vibration containing multiple shocks. 2004
5. Dong RG, Welcome DE, McDowell TW, Xu XS, Krajnak K, Wu JZ. A proposed theory on biodynamic frequency weighting for hand-transmitted vibration exposure. Industrial Health. 2012; 50(5):412–424. [PubMed: 23060254]
6. Kim TH, Kim YT, Yoon YS. Development of a biomechanical model of the human body in a sitting posture with vibration transmissibility in the vertical direction. International Journal of Industrial Ergonomics. 2005; 35:817–829.
7. Nawayseh N, Griffin MJ. A model of the vertical apparent mass and the fore-and-aft cross-axis apparent mass of the human body during vertical whole-body vibration. Journal of Sound and Vibration. 2009; 319(1–2):719–730.
8. Wei L, Griffin MJ. Mathematical models for the apparent mass of the seated human body exposed to vertical vibration. Journal of Sound and Vibration. 1998; 212(5):855–874.
9. Dong RG, Dong JH, Wu JZ, Rakheja S. Modeling of biodynamic responses distributed at the fingers and the palm of the human hand–arm system. Journal of Biomechanics. 2007; 40:2335–2340. [PubMed: 17166500]
10. Cherian T, Rakheja S, Bhat RB. An analytical investigation of an energy flow divider to attenuate hand-transmitted vibration. International Journal of Industrial Ergonomics. 1996; 17:455–467.
11. Wu JZ, Dong RG, Welcome DE, Xu XS. A method for analyzing vibration power absorption density in human fingertip. Journal of Sound and Vibration. 2010; 329:5600–5614.
12. Hinz B, Menzel G, Blüthner R, Seidel H. Transfer functions as a basis for the verification of models – variability and restraints. Clinical Biomechanics. 2001; 16(Suppl. 1):S93–S100. [PubMed: 11275347]
13. Green PL, Worden K, Sims ND. On the identification and modelling of friction in a randomly excited energy harvester. Journal of Sound and Vibration. 2013; 332:4696–4708.

14. Dong RG, Pan CS, Hartselle JJ, Welcome DE, Lutz T, Brumfield A, Harris JR, Wu JZ, Wimer B, Mucino V, Means K. An investigation on the dynamic stability of scissor lift. The Open Journal of Safety Science and Technology. 2012; 2:8–15.
15. Dong RG, Welcome DE, McDowell TW, Wu JZ. Modeling of the biodynamic responses distributed at the fingers and palm of the hand in three orthogonal directions. Journal of Sound and Vibration. 2013; 332:1125–1140. [PubMed: 26609187]
16. Jahn R, Hesse M. Application of hand-arm models in the investigation of the interaction between man and machine. Scandinavian Journal of Work, Environment & Health. 1986; 12:343–346.
17. Kinne, J.; Latzel, K.; Schenk, TH. Application of two-hand impedance as basis for mechanical modeling; Proceedings of the Ninth International Conference on Hand–Arm Vibration; Nancy, France. 2001. p. 113-118.
18. Dong RG, McDowell TW, Welcome DE, Warren C, Wu JZ, Rakheja S. Analysis of anti-vibration gloves mechanism and evaluation methods. Journal of Sound and Vibration. 2009; 321:435–453.
19. Mozaffarin A, Pankoke S, Wölfel H-P. MEMOSIK V – an active dummy for determining three-directional transfer functions of vehicle seats and vibration exposure ratings for the seated occupant. International Journal of Industrial Ergonomics. 2008; 38:471–482.
20. Dong RG, Welcome DE, Wu JZ, McDowell TW. Development of hand–arm system models for vibrating tool analysis and test rig construction. Noise Control Engineering Journal. 2008; 56(1): 35–44.
21. Freivalds, A. Biomechanics of the Upper Limbs – Mechanics, Modeling, and Musculoskeletal Injuries. New York: CRC Press; 2004.
22. Dong RG, Welcome DE, McDowell TW, Wu JZ. Theoretical relationship between vibration transmissibility and driving-point response functions of the human body. Journal of Sound and Vibration. 2013; 332(24):6193–6202. [PubMed: 26663932]
23. Griffin MJ. The validation of biodynamic models. Clinical Biomechanics Supplement 1. 2001:S81–S92.
24. Adewusi S, Rakheja S, Marcotte P. Biomechanical models of the human hand – arm to simulate distributed biodynamic responses for different postures. International journal of Industrial Ergonomics. 2012; 42:249–260.
25. Amirouche FML, Ider SK. Simulation and analysis of a biodynamic human model subjected to low accelerations – a correlation study. Journal of Sound and Vibration. 1988; 123:281–292.
26. Fritz M. An improved biomechanical model for simulating the strain of the hand–arm system under vibration stress. Journal of Biomechanics. 1991; 21:1165–1171. [PubMed: 1769981]
27. Boileau P-É, Rakheja S, Wu X. A body mass dependent mechanical impedance model for applications in vibration seat testing. Journal of Sound and Vibration. 2002; 253(1):243–264.
28. Pankoke S, Buck B, Wölfel HP. Dynamic FE model of sitting man adjustable to body height, body mass and posture used for calculating internal forces in the lumbar vertebral disks. Journal of Sound and Vibration. 1998; 215:827–839.
29. Wu JZ, Dong RG, Smutz WP, Schopper AW. Nonlinear and viscoelastic characteristics of skin under compression: experiment and analysis. Biomedical Material Engineering. 2003; 13(4):373–385.
30. Kihlberg S. Biodynamic response of the hand – arm system to vibration from an impact hammer and a grinder. International Journal of Industrial Ergonomics. 1995; 16:1–8.
31. Dong JH, Dong RG, Rakheja S, Welcome DE, McDowell TW, Wu JZ. A method for analyzing absorbed power distribution in the hand and arm substructures when operating vibrating tools. Journal of Sound and Vibration. 2008; 311:1286–1309.
32. Harris, CM. Shock and Vibration Handbook. fourth. New York: McGraw-Hill; 1995.
33. Worden K, Manson G. On the identification of hysteretic systems. Part I: fitness landscapes and evolutionary identification. Mechanical Systems and Signal Processing. 2012; 29:201–212.
34. Worden K, Staszewski WJ, Hensman JJ. Natural computing for mechanical systems research: a tutorial overview. Mechanical Systems and Signal Processing. 2011; 25(1):4–111.
35. Tregoubov VP. Problems of mechanical model identification for human body under vibration. Mechanism and Machine Theory. 2000; 35:491–504.

36. Dong RG, Rakheja S, McDowell TW, Welcome DE, Wu JZ. Estimation of the biodynamic responses distributed at fingers and palm based on the total response of the hand–arm system. International journal of Industrial Ergonomics. 2010; 40(4):425–436.

37. Dong RG, Welcome DE, McDowell TW, Wu JZ. Measurement of biodynamic response of human hand – arm system. Journal of Sound and Vibration. 2006; 294(4–5):807–827.

38. Welcome DE, Dong RG, Xu XS, Warren C, McDowell TW, Wu JZ. An investigation on the 3-D vibration transmissibility on the human hand–arm system using a 3-D scanning laser vibrometer. Canadian Acoustics. 2011; 39(2):44–45.

39. Wang W, Rakheja S, Boileau P-É. Relationship between measured apparent mass and seat-to-head transmissibility responses of seated occupants exposed to vertical vibration. Journal of Sound and Vibration. 2008; 314:907–922.

40. Rakheja S, Dong RG, Patra S, Boileau P-É, Marcotte P, Warren C C. Biodynamics of the human body under whole-body vibration: synthesis of the reported data. International Journal of Industrial Ergonomics. 2010; 40:710–732.

41. Welcome DE, Dong RG, Xu XS, Warren C, McDowell TW. The effects of vibration-reducing gloves on finger vibration. International Journal of Industrial Ergonomics. 2014; 44:45–59. [PubMed: 26543297]

42. Dong RG, Welcome DE, McDowell TW, Wu JZ, Schopper AW. Frequency weighting derived from power absorption of fingers–hand–arm system under z_h-axis. Journal of Biomechanics. 2006; 39:2311–2324. [PubMed: 16154576]

43. Xu XS, Welcome DE, McDowell TW, Wu JZ, Wimer B, Warren C, Dong RG. The vibration transmissibility and driving-point biodynamic response of the hand exposed to vibration normal to the palm. International Journal of Industrial Ergonomics. 2011; 41(5):418–427.

44. Thomas M, Beauchamp Y. Development of a new frequency weighting filter for the assessment of grinder exposure to wrist transmitted vibration. Computers & Industrial Engineering. 1998; 35(3–4):651–654.

45. Dong RG, Sankar S, Dukkipati PV. A finite element model of railway track and its application to wheelflat problem. Proceedings of the Institution of Mechanical Engineers. 1994; 208(Part F):61–72.

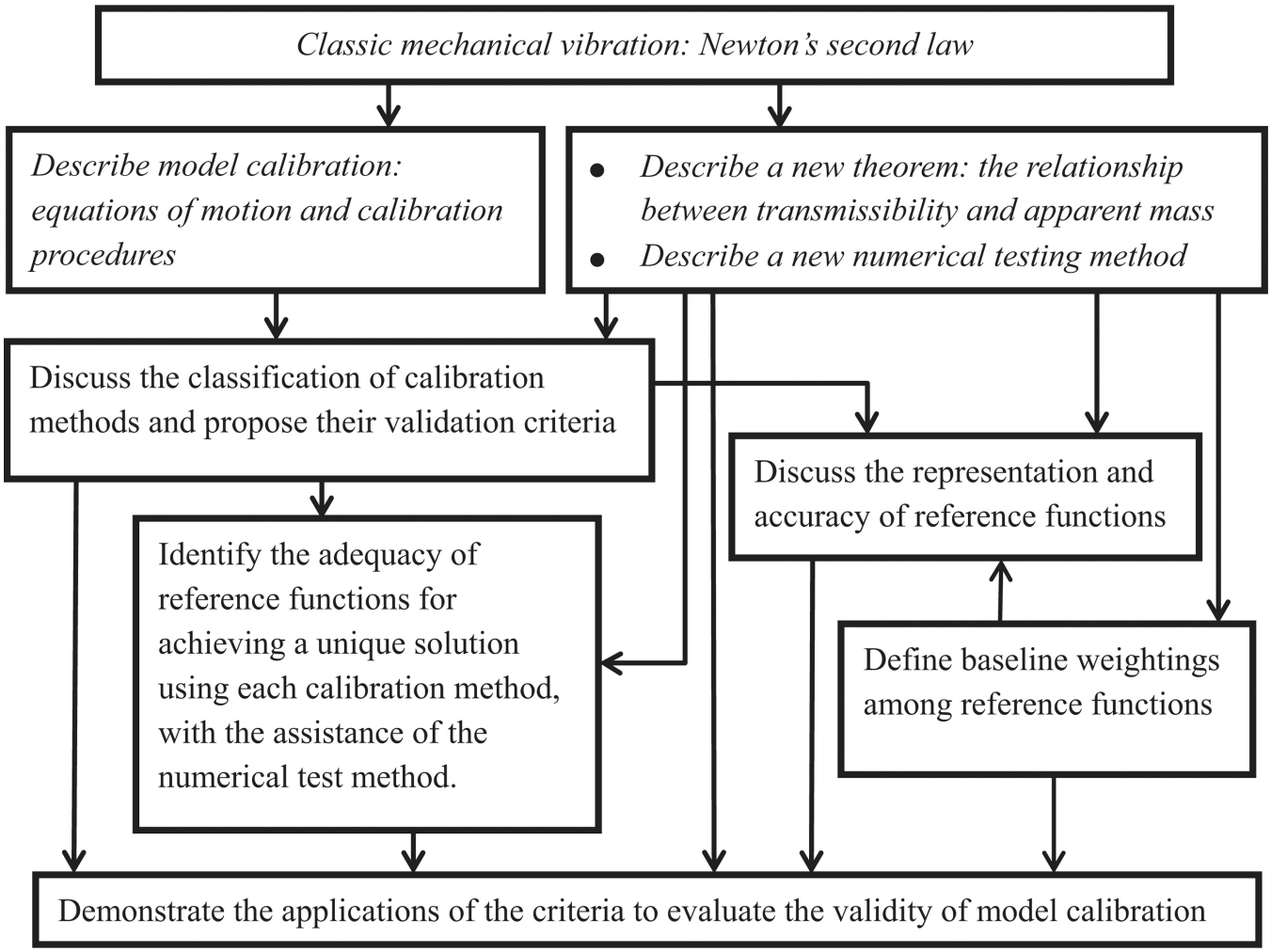

Fig. 1.
A flowchart showing the methods and major activities of this study.

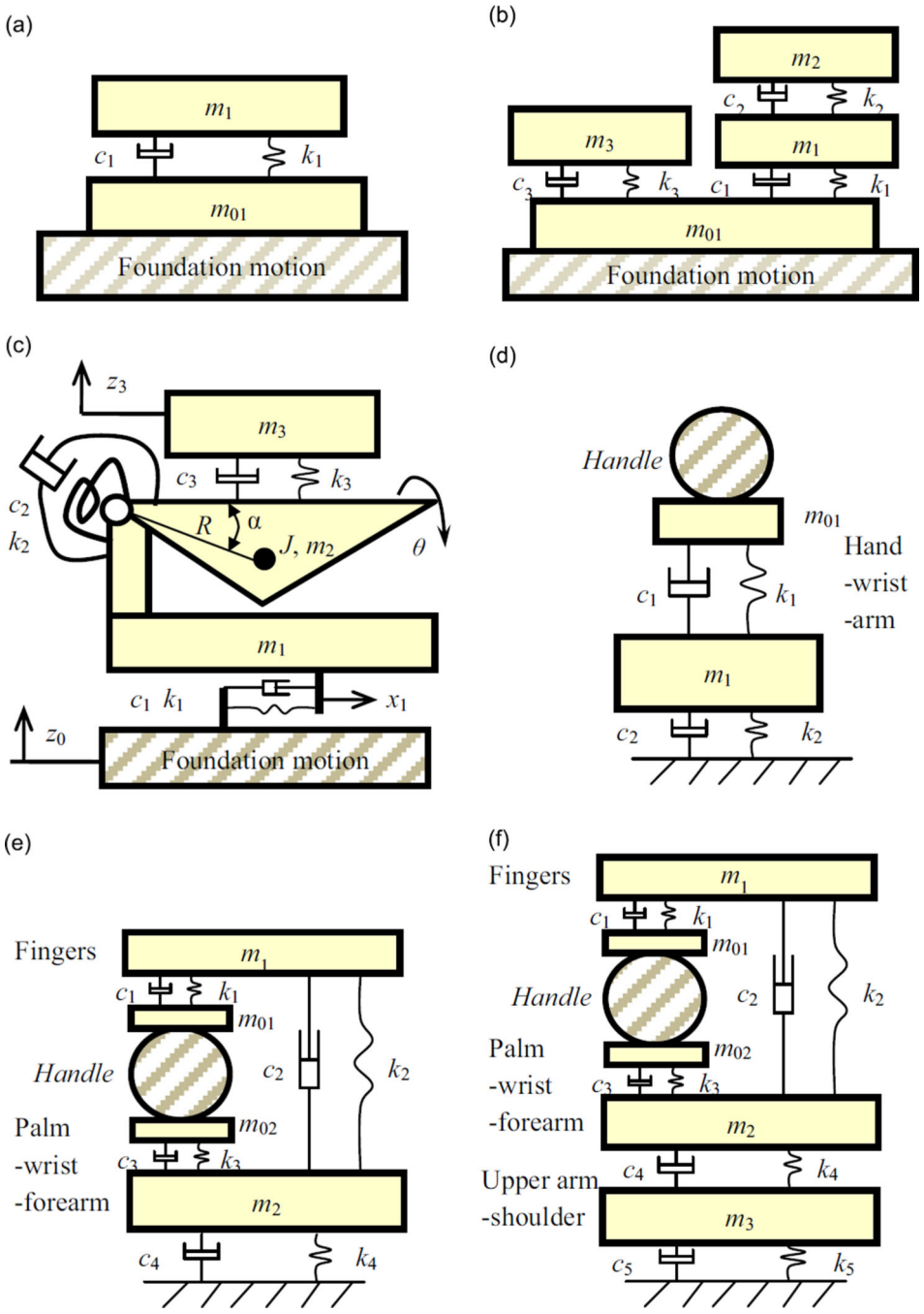

Fig. 2.

Six models of the human body vibration: (a) 1-dof whole-body model [8]; (b) 3-dof whole-body model [27]; (c) 3-dof whole-body fore-aft responses model [7]; (d) 1-dof hand-arm model [20]; (e) 2-dof hand-arm model [9]; and (f) 3-dof hand-arm model [9].

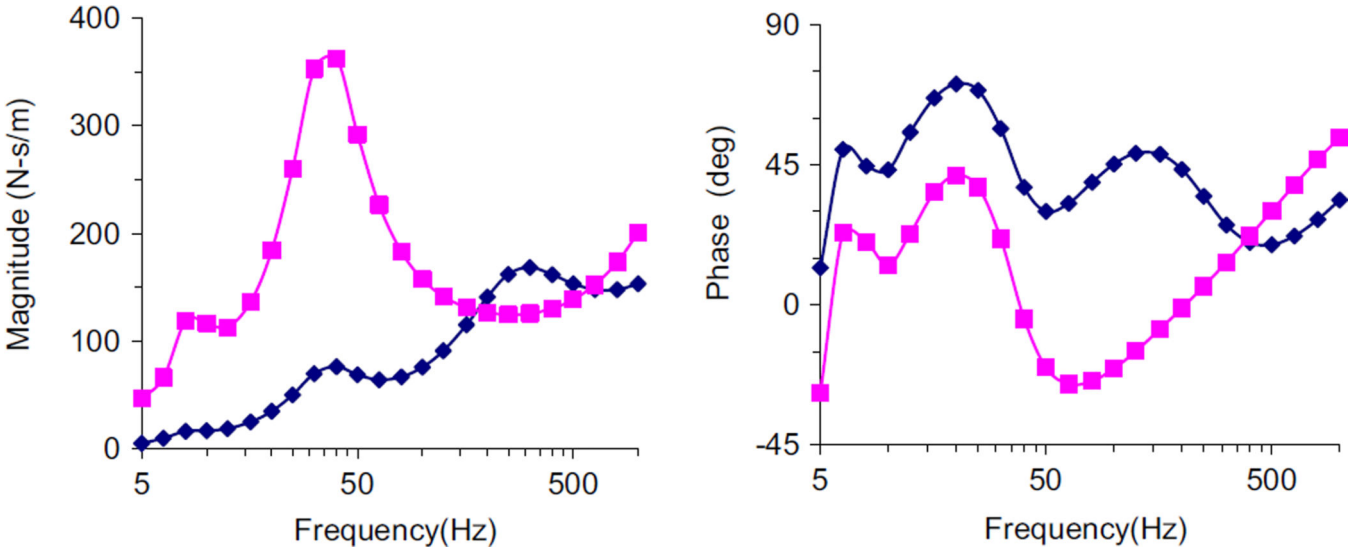

Fig. 3.

The mechanical impedances ($Z=\omega j \cdot M$) distributed at the fingers and the palm of the hand, which are calculated from Model-(f) using the parameters listed in Table 1 (palm; fingers).

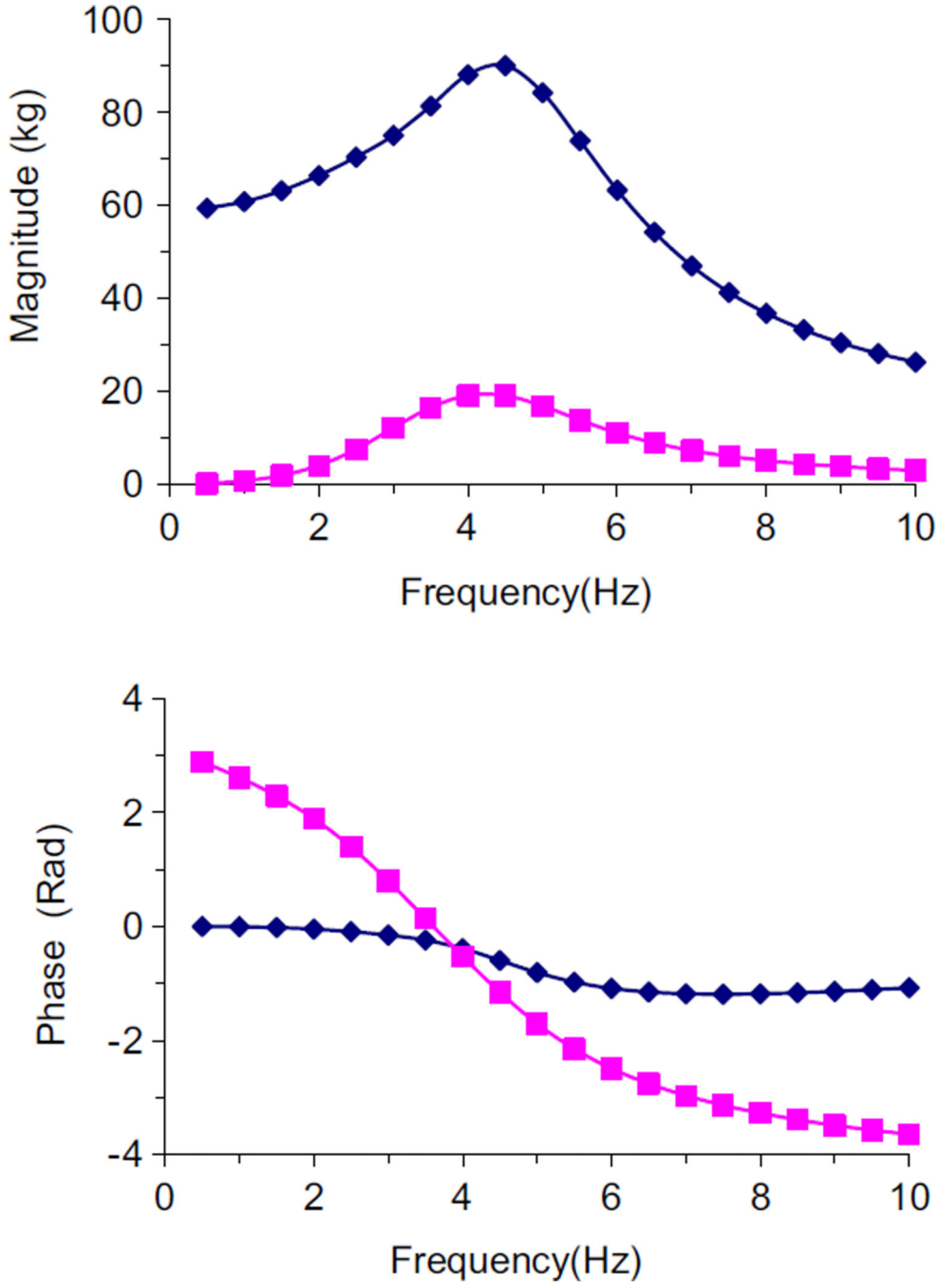

Fig. 4.

The vertical apparent mass and fore-and-aft cross-axis apparent mass of the human body subjected to vertical whole-body vibration, which are calculated from Model-(c) using the parameters in Table 1 (cross-axis apparent mass fore-aft direction; apparent mass in vertical direction).

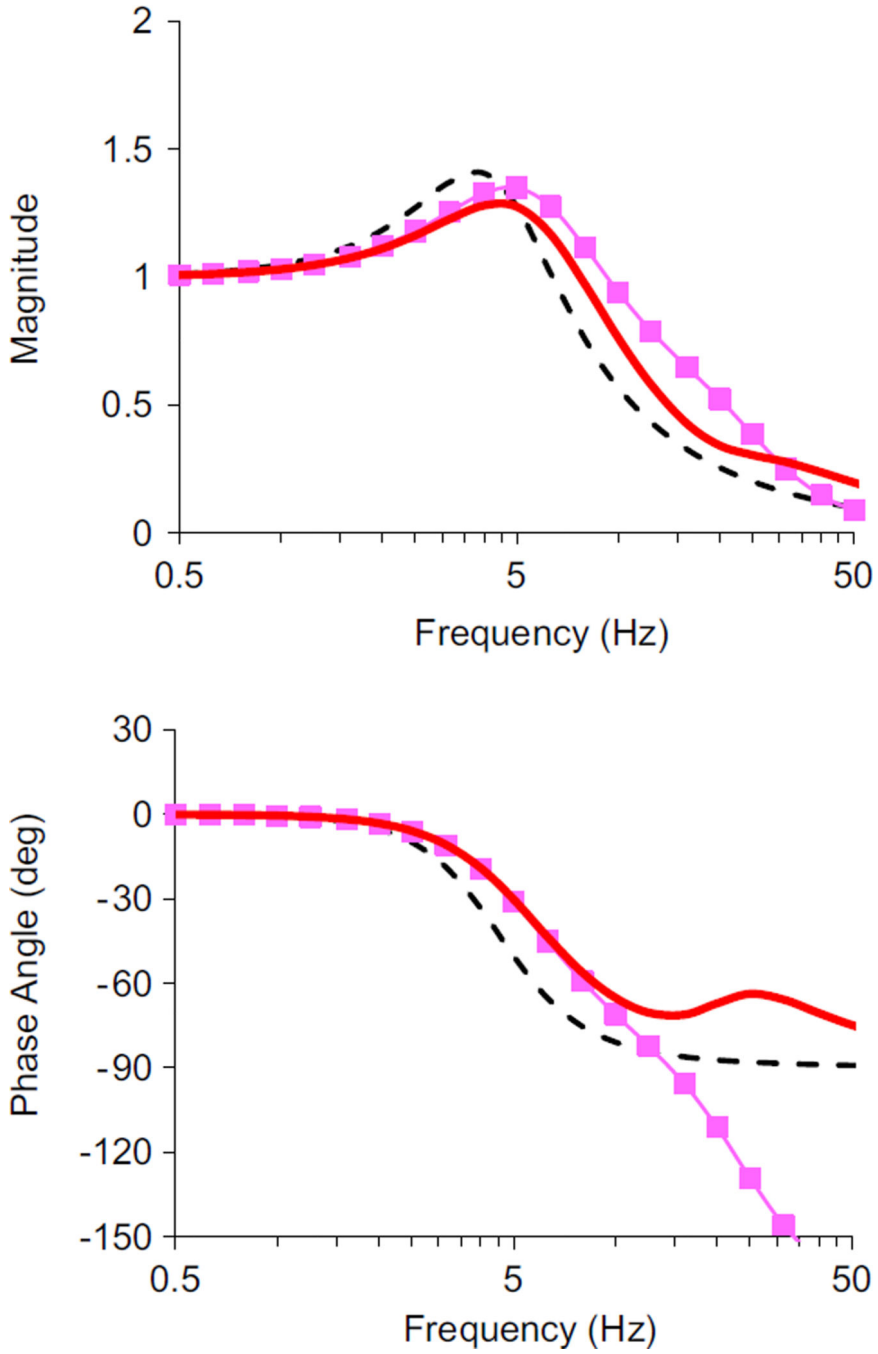

Fig. 5.

The comparisons of the three transmissibility functions of Model-(b) for simulating whole-body vibration, which are calculated using the parameters in Table 1 (—— T_1; T_2; – – – T_3).

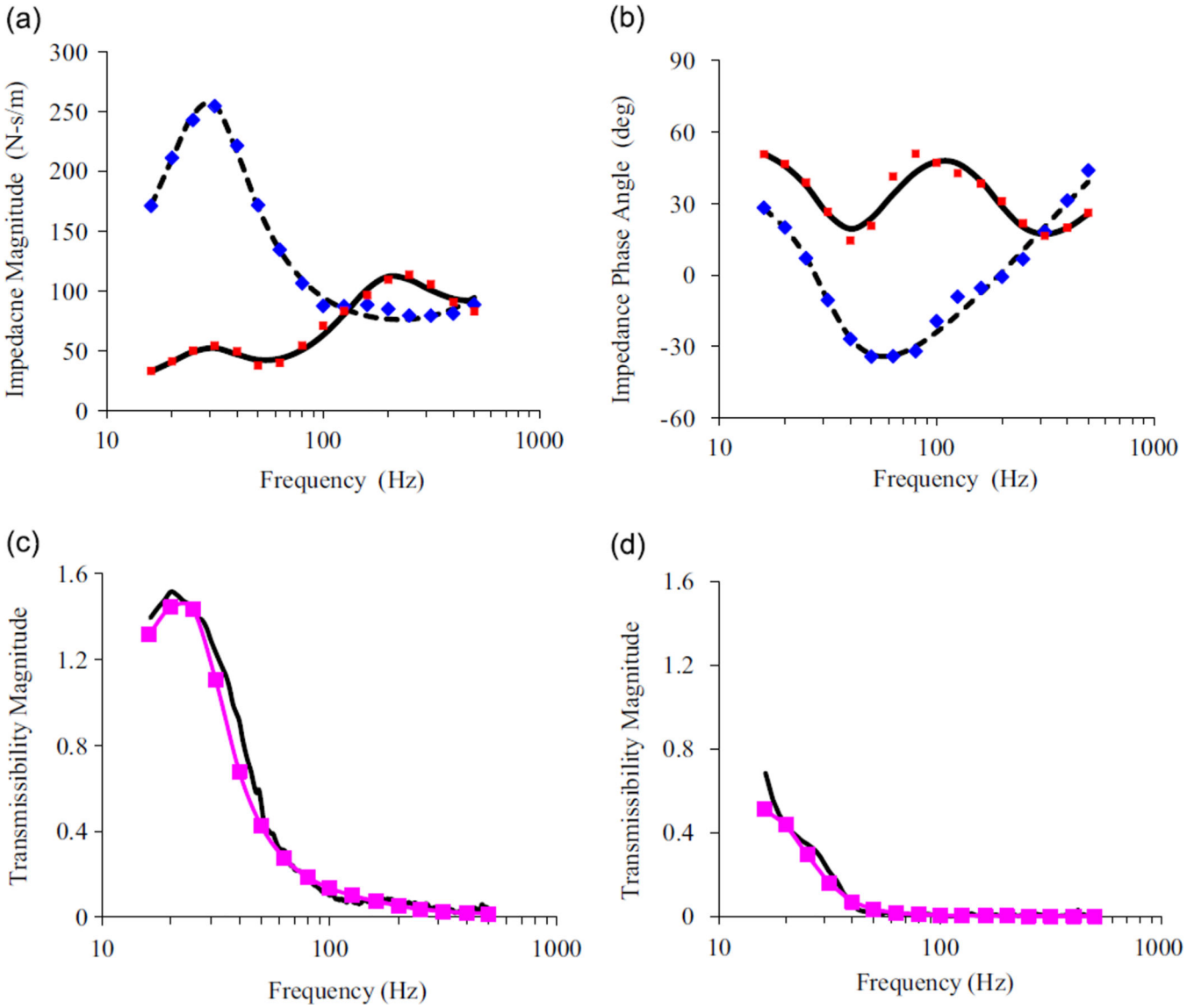

Fig. 6.

Comparisons of the modeling and experimental data of the frequency response functions along the forearm (*z*) direction of the hand-arm system [15]: (a) mechanical impedance magnitude; (b) mechanical impedance phase angle; (■ experiment_fingers; ——— modeling_fingers; ◆ experiment_palm; - - - - modeling_palm); (c) transmissibility at the wrist; and (d) transmissibility on the upper arm; (■——■ modeling prediction; — experiment data).

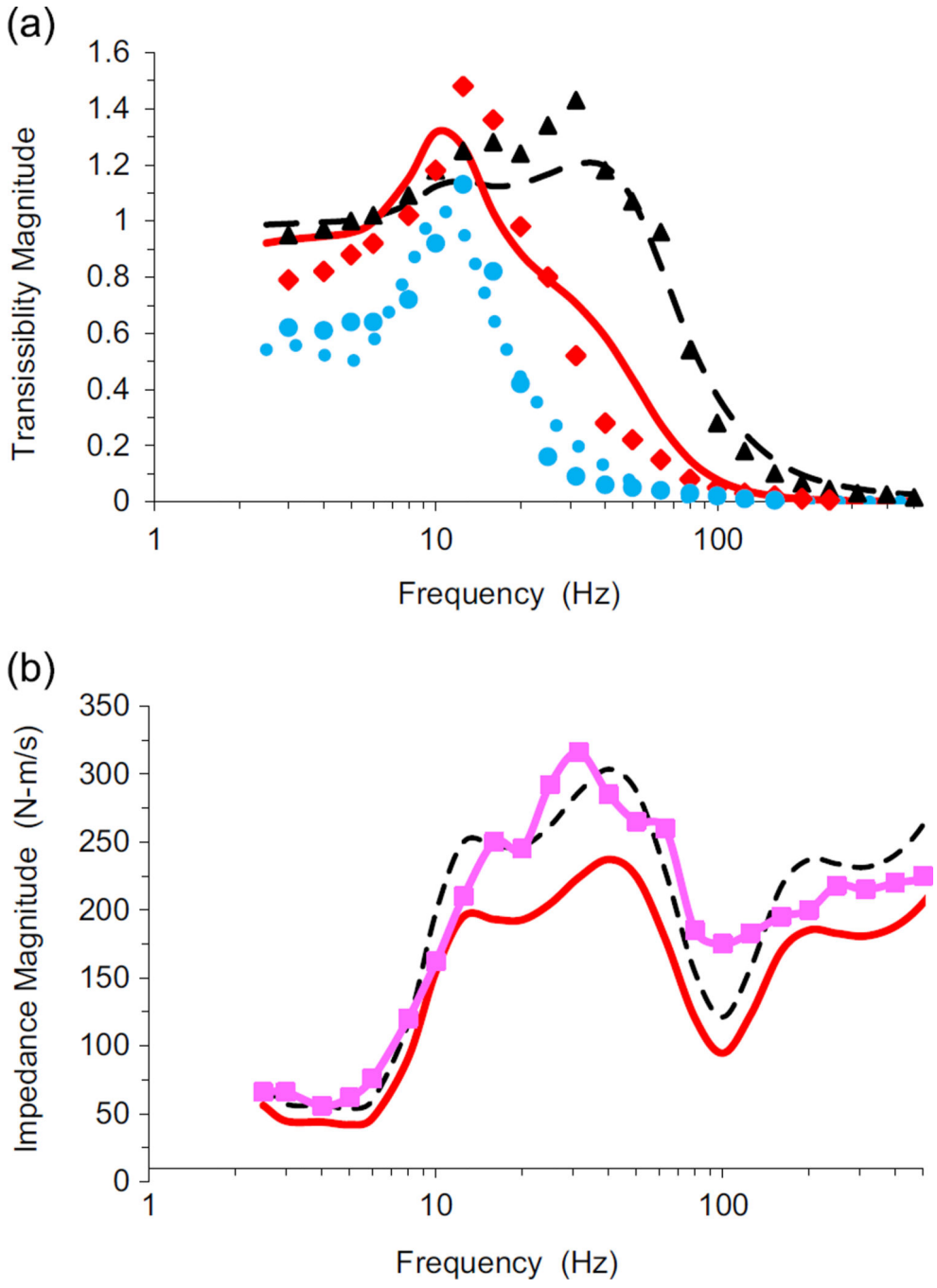

Fig. 7.

The comparisons of the modeling predictions and measured response functions presented in a reported study (bent arm model) [24], in which the hand model structure is similar to that of Model-(f): (a) transmissibility functions (▲ experiment_wrist; – – – model_palm; ♦ experiment_forearm; ——— model_forearm; ✸ experiment_upper arm; ····· model_upper arm); (b) impedance data (——— original modeling impedance; ——■——— measured impedance; – – – modeling impedance with the original parameters increased by 28%).

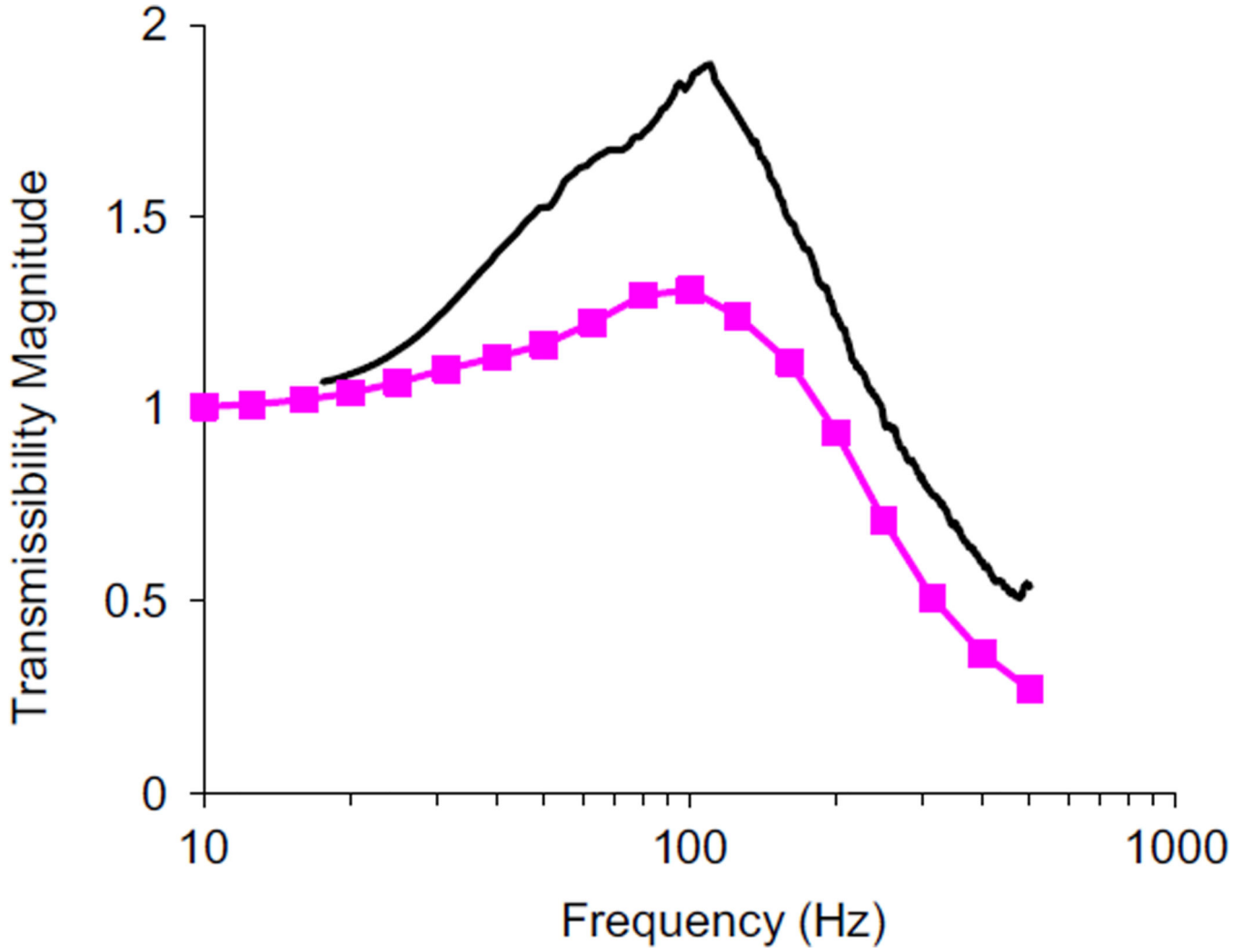

Fig. 8.

The comparison of the modeling and measured transmissibility functions of the total vibration (the vector sum of the three-axis vibrations) on the fingers under combined 30 N grip and 50 N push action: modeling prediction [15]; experiment data [41].

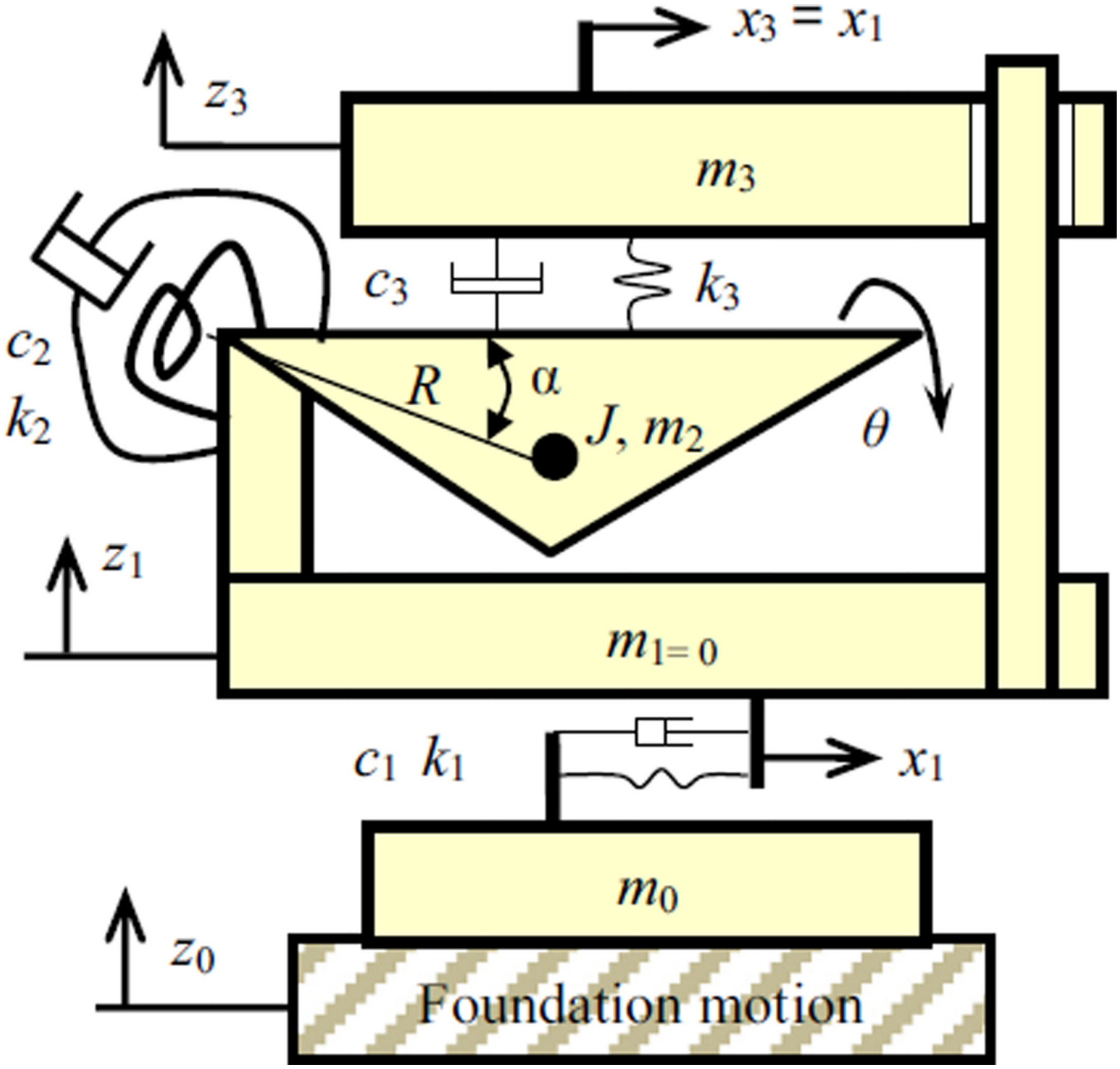

Fig. 9.
Proposed revision of Model-(c)

Table 1

The reference parameter values for the models shown in Fig. 2, which are taken from the reported studies [7–9,20,27]. As also shown in Fig. 2, m is component mass; c is damping property; k is stiffness; J, R and α are the three rotational parameters of m_2 in Model-c, which respectively present the inertia moment of the mass, its rotational arm length, and the angular position of the mass center on rotational arm [7].

Parameter ID	Unit	Model ID and data source					
		(a) [8]	(b) [27]	(c) [7]	(d) [20]	(e) [9]	(f) [9]
m_{01}	kg	4.1	2.0		0.049	0.014	0.014
m_{02}	kg					0.027	0.027
m_1	kg	46.7	6.0	0.0	1.555	0.082	0.082
m_2	kg		2.0	18.0		1.415	1.420
m_3	kg		45.0	41.0			6.089
J	kg m^2			0.2			
k_1	N/m	44115	9990	33355	62804	207964	208489
k_2	N/m		34400	88	4279	6523	6347
k_3	N/m		36200	43441		58555	57535
k_4						4207	5382
k_5							9425
c_1	N s/m	1522	387	659	192.9	120.8	120.6
c_2	N s/m		234	7	76.1	37.9	38.0
c_3	N s/m		1390	660		118.3	118.4
c_4	N s/m					85.9	77.0
c_5	N s/m						97.5
R	M			0.11			
α	Rad			1.26			
Frequency range used in this study (Hz)		0.5 – 20	0.5 –20	0.5 – 10	10 – 1000	16 – 1000	5 – 1000

Table 2

Comparisons of the reference parameter values for Model-(c) [7] with three alternative solution values identified from the numerical tests of the current study (% Error = 100*[$P-P_{Ref}$]/P_{Ref}).

Parameter	Unit	Reference value	Alternative 1		Alternative 2		Alternative 3	
			Value	% Error	Value	% Error	Value	% Error
m_1	kg	0.0	1.573748	∞	0	0.0	0	0.0
m_2	kg	18.0	17.44799	3.1	18	0.0	18	0.0
m_3	kg	41.0	40.12633	2.1	41	0.0	41	0.0
J	kg m^2	0.2	0.145926	27.0	0.5	−150.0	9.41	−4605.0
k_1	N/m	33355	32781.9	1.7	33355	0.0	33355	0.0
k_2	N m/Rad	88	67.59272	23.2	220	−150.0	4140.4	−4605.0
k_3	N/m	43441	42672.08	1.8	43441	0.0	43441	0.0
C_1	N s/m	659	696.4224	−5.7	659	0.0	659	0.0
C_2	N m s/Rad	7	5.455718	22.1	17.5	−150.0	329.35	−4605.0
C_3	N s/m	660	575.9485	12.7	660	0.0	660	0.0
R	m	0.11	0.092443	16.0	0.173925	−58.1	0.754523	−585.9
α	Rad	1.26	1.209114	4.0	1.26	0.0	1.26	0.0
Goodness of the curve fitting			r^2 > 0.9999 Error = 2.7		r^2 = 1.0000 Error = 0.0000		r^2 = 1.0000 Error = 0.0000	

Table 3

Comparisons of the reference parameter values for Model-(b) [27] with three alternative solution values identified from the numerical tests of the current study (% Error = 100*[$P-P_{Ref}$]/P_{Ref}).

Parameter	Unit	Reference value	Alternative 1		Alternative 2		Alternative 3	
			Value	% Error	Value	% Error	Value	% Error
m_{01}	kg	2.0	1.86	−7.1	1.92	−4.0	2.16	7.9
m_1	kg	6.0	7.20	20.0	6.60	10.0	4.80	−20.0
m_2	kg	2.0	2.40	20.0	2.20	10.0	1.60	−20.0
m_3	kg	45.0	43.10	−4.2	44.10	−2.0	46.79	4.0
k_{12}	N/m	9990	11988	20.0	10989	10.0	7992	−20.0
k_{21}	N/m	34400	41280	20.0	37840	10.0	27520.	−20.0
k_3	N/m	36200	34670	−4.2	35476	−2.0	37643	4.0
c_1	N s/m	387	464.4	20.0	425.7	10.0	309.6	−20.0
c_2	N s/m	234	280.8	20.0	257.4	10.0	187.2	−20.0
c_3	N s/m	1390	1331.3	−4.2	1362.2	−2.0	1445.4	4.0
Goodness of the curve fitting			$r^2 \geq 0.9996$ Error = 19.0		$r^2 \geq 0.9999$ Error = 9.3		$r^2 \geq 0.9996$ Error = 18.6	